J Mater Sci (2010) 45:287–325
DOI 10.1007/s10853-009-3995-5

REVIEW

The rapid solidification processing of materials: science, principles, technology, advances, and applications

Enrique J. Lavernia · T. S. Srivatsan

Received: 26 August 2009 / Accepted: 26 October 2009 / Published online: 1 December 2009

Abstract The purpose of this technical manuscript is to present an explanation of rapid solidification processing in an easily understandable manner so that the technique is widely accepted and put to commercial practice by many working in the industries of materials processing and manufacturing engineering. The comprehensive review article presents a comprehensive overview of the widely accepted and used rapid solidification processes. To better, understand rapid solidification in comparison with conventional solidification, the intrinsic aspects and types of nucleation and the kinetics governing nucleation and subsequent growth of the crystal during rapid solidification are presented and discussed. The commercially viable methods for the rapid solidification processing of metal-based and even intermetallic-based composites are presented. The technically viable methods for the consolidation of rapidly solidified powders are discussed. A succinct description of notable recent advances in the technique of spray processing is presented. In the last section of this article, we highlight the key findings of selected studies in the area of rapid solidification processing of advanced metallic, intermetallics, and composite materials that have helped to advance the processing technique for emerging applications that is synchronous with advances in technology.

E. J. Lavernia
University of California, Davis, One Shields Avenue,
Davis, CA 95616-8558, USA
e-mail: lavernia@ucdavis.edu

T. S. Srivatsan (✉)
Division of Materials Science and Engineering, Department of Mechanical Engineering, The University of Akron,
Akron, OH 44325-3903, USA
e-mail: tsrivatsan@uakron.edu

Introduction

Rapid solidification (RS) is "loosely" defined in the scientific literature as the rapid extraction of thermal energy to include both superheat and latent heat during the transition from a liquid state at high temperatures, to solid material at room or ambient temperature. The rapid extraction of heat can cause undercoolings as high as 100 °C or more prior to the initiation of solidification. This is in direct comparison to the few degrees obtained for the case of conventional casting about 1 °C or less per second. For a process to be considered in the RS regime, the cooling rate would have to be of the order greater than 10^4 K/s although cooling rates of 10^3 K/s sometimes generate rapidly solidified microstructures. The time of contact at high temperatures is limited to milli-seconds followed by rapid quenching to room temperature. The choice of the quenching medium, be it water, brine solution, or liquid nitrogen, has a profound influence on solidification rate and the resultant microstructural development to include the distribution of second-phases in the final product. The high-cooling rate results in a significant amount of undercooling of the melt, which is conducive for the occurrence of several metastable effects that can be categorized as being either constitutional or microstructural.

The rapid extraction of thermal energy that occurs during RS permits large deviations from equilibrium, which offers the salient advantages of:

(i) an extension of solid solubility, often by orders of magnitude;
(ii) enhanced compositional flexibility;
(iii) formation of non-equilibrium or metastable crystalline phases from the melt through alternate phase selection processes and/or an incorporation of

desirable second-phases like fine dispersoids and ductile particles;
(iv) a reduction in both the number and size of segregated phases;
(v) retention of disordered crystalline structure in normally ordered materials and intermetallic compounds;
(vi) the intrinsic microstructural effects include either one or a combination of changes in grain morphology, refinement of features, such as, the size and shape of grains, and the shape and location of the phases present.

Of course, it is likely that not all of these advantages occur concurrently. However, rapid cooling of the molten metal, through the solidification temperature range, is achieved by ensuring that solidification occurs with as small a cross-sectional dimension of the molten metal that is in thermal contact with an effective heat sink.

Most importantly, there are at least four different cooling regions, which must be considered [1]:

(a) in the liquid metal from the melt temperature to a temperature at which nucleation and growth of crystals or the formation of glass occurs;
(b) during the growth and solidification process;
(c) through post-solidification cooling, which occurs upon contact with a solid substrate or on a fluid medium;
(d) following separation from a substrate, if appropriate.

In general, it is the cooling rate during solidification, which has the single most important influence on microstructural refinement. However, in a few instances, the degree of undercooling prior to crystallization is very important, and the post-solidification cooling rate does affect the resultant microstructure through the conjoint influences of solid-state diffusion and coarsening processes.

The late Professor Paul Duwez undertook early investigations related to rapid quenching of metals and their alloy counterparts from the liquid state. His first report in 1960 heralded a new era in physical metallurgy by identifying novel constitutional and microstructural effects that are achievable through RS [2–4]. The development, emergence, and commercialization of rapid solidification techniques (RST), in the 1970s, to produce long and continuous tapes and ribbons of near uniform cross-section provided the desired impetus for noticeable advances in this rapidly developing field. The decade of the 1980s witnessed additional breakthroughs in the design and development of alloys having novel compositions, refined microstructures, and improved physical and mechanical properties. Over four decades, i.e., since the 1970s, of sustained research activity associated with the effects of RS and its products resulted in the emergence of a spectrum of solidification techniques that yielded a range of products.

This review article provides an explanation of RSP and a discussion of the viable RST for the processing of metal, intermetallic, and even composites based on metal and intermetallic matrices. A classification of the RS processes are presented, and salient aspects of the single splat process, the continuous process, the atomization process, and the self-quench process are highlighted. The intrinsic aspects and types of nucleation along with an overview of the kinetics governing nucleation and crystal growth during solidification are presented and discussed. The second part of this article discusses the economically viable methods in current use for RSP of composite materials. The key processes related to consolidation of the rapidly solidified powders to dense bodies are introduced and discussed. In the following section, we provide an overview of advances in spray processing techniques. We conclude with a section that highlights selected examples taken from recent studies.

Rapid solidification processing

The technology of rapid solidification processing (RSP) has, since its emergence, made noticeable, yet significant advancements to becoming a potent and compelling fabrication technique as evident by the number of books and monographs [5–12], numerous conferences and symposia [13–19], and specialized topical reviews [1, 20–28] dedicated to the advancement of this subject. As apparent from the work documented in these references and Table 1, rapid solidification encompasses a broad spectrum of technologies from atomization techniques for the production of powder to plasma spray processes for the production of coatings. As renewed interest in advanced metallic, the family of intermetallic, and even discontinuously reinforced composite materials based on either metal or intermetallic matrices grew in strength, the processing of these new and improved materials and the field of RSP began to synergize and blend with each other. With time, the techniques of RSP have emerged with strength and progressively grown in stature to become an integral part of the fabrication scheme for metal-based, intermetallic-based, and even ceramic-based composites.

From a practical viewpoint, there are at least three different ways to achieve rapid solidification [29]:

(1) imposing a high degree of undercooling prior to solidification;
(2) imposing a high velocity of advance during continuous solidification;
(3) imposing a high-cooling rate during solidification.

Table 1 Rapid solidification techniques [79]

Process name	Description	Product/dimensions	Cooling rate (K s^{-1})
Atomization methods			
Fluid atomization (normally twin jets)	High-pressure fluid impacting a continuous stream of liquid metal	For gas : low O_2 contamination	Gas: 10^2–10^3
		Spherical and smooth powder 50/100 μm dia	SSGA: up to 10^6
Gas (Ar, N_2)	Ultrasonic G.A: disintegration occurs by high intensity pulsed waves	Supersonic G.A: 10–50 μm	USGA: 10^5
		Ultrasonic G.A: <30 μm	
Water		For water: high O_2 contamination	Water: 10^2–10^4
		Irregular particulates 75/200 μm dia	
Vacuum atomization (soluble gas)	Molten metal supersaturated with gas under pressure is suddenly exposed to vacuum, gas expands causing liquid to atomize	Spherical powder 40/150 μm dia	10^4–10^5
Drum splat quenching	Gas atomized droplets directed to impinge on a rotating drum	Flakes 50/100 μm thick 1–3 mm dia	10^4–10^5
Rotating electrode process (REP)	Alloy in electroded form is rotated (250 rps) while being melted by an arc plasma/bean. Molten metal is ejected centrifugally and solidified in an inert gas filled chamber	Spherically/smooth powder 150/200 μm dia	10^2
Rapid solidification rate (RSR) (centrifugal atomization)	Molten metal is ejected into a rotating water-cooled cup/disc resulting in fine droplets cooled by high flow helium gas	Spherical powder <100 μm dia	10^5
Twin roll atomization	Mechanical atomization process where stream of molten metal is directed into a high speed contra rotating rolls	Variable powder/flake 200 μm thick	10^5–10^6
Laser melting/spin atomization	Focused (CO_2) laser beam is used to melt the top of the rotating rod. Droplets are expelled by the centrifugal force and cooled by the inert gas	Spherical particles 40 μm dia	$\gg 10^4$
Electrohydrodynamic atomization (EHDA)	Electric field is applied to the surface of liquid metal and causes a droplet to be emitted	Droplets > 0.01–150 μm dia	10^7
Spark erosion technique	Repetitive spark discharge between two electrodes immersed in a dielectric fluid. Spark vaporizes a small amount of metal that immediately freezes	$\gg$0.5 μm dia contamination from dielectric fluid	10^5–10^6
Electron bean meting combined with spat quenching (EBSO)	A focused electron beam melts the bottom tip, molten drops fall onto the surface of a rotating disc	Flakes 50 mm dia 50 μm thick	10^6
Chilling methods			
Melt spinning (CBMS)	Molten metal is expelled out onto a rotating wheel (flat or notched)	Ribbons thick 25/50 μm	10^5–10^7
Crucible melt extraction (CME)	Molten metal solidifies on the edge of a water-cooled disc and flies off	Filaments or fibers 20–100 μm thick	10^5–10^6
Melt drag (overflow)	Overflow of a molten metal from a reservoir onto a chill rotating surface	Filaments, foils, particulates	10^4–10^6
Pendant drop (POME)	Filament is extracted from molten end of a rod suspended just above the rotating wheel	Filaments, fibers	10^5–10^6

Table 1 continued

Process name	Description	Product/dimensions	Cooling rate (K s^{-1})
Rapid spinning cap (RSC)	Stream of molten metal is ejected onto a thick layer of rotating liquid located in the interior wall of a spanning cup	Spherical to irregular powder/flakes 50 mm dia 50 μm thick	10^6
Plasma and anvil twin pistons	Droplet of molten metal is impacted by piston(s)	Splat 5–300 μm thick	10^4–10^6
Plasma spray deposition	Molten metal is propelled onto a substrate by a hot ionized gas emanating from the plasma torch. If deposited layers are kept very thin, rapid solidification is possible. Potential for near net shape. Coherent deposit	Porous layer >50 μm thick	10^3–10^6
Arc spray	Electrically opposed charged wires of the alloy to be sprayed are fed together to produce a controlled arc. The molten metal is atomized and by a stream of gas is projected onto a substrate	Porous film >50 μm thick	10^2–10^5

The first approach involves supercooling a volume of melt to a temperature at which the latent heat released during solidification is completely dissipated through the solidifying volume, prior to being transferred to the surroundings. The concept of undercooling is illustrated in the schematic shown in Fig. 1 [30]. In this figure, the composition C_O is undercooled into a single-phase region. With a progressive increase in temperature achieved during the release of latent heat of solidification (referred to as "recalescence"), it returns to the two-phase ($\alpha + L$) region. In Fig. 1b is shown how the process of recalescence helps bring the temperature back to precisely the solidus temperature (T_S). This condition is referred to as "critical undercooling" ($T_R = T_S$). In Fig. 1c is shown how the recalescence aids in bringing the temperature into the single-phase region. This condition is termed as "hypercooling" ($T_R < T_S$).

In the absence of heat transfer to the adjacent surroundings, the temperature of the solidifying volume increases during recalescence by an amount equivalent to C/L, where C is the specific heat of the solid and L is the latent heat of solidification per unit mass. Hence, in order to achieve "hypercooling," the initial amount of undercooling (ΔT) below the equilibrium liquidus must be sufficient to exceed the rise in temperature (C/L). In practice, several experimental techniques have been developed to control the range of undercoolings prior to solidification. The accepted and most widely used techniques include the following:

(a) the droplet emulsion technique (DE) [31];
(b) the drop tube technique (DT) [32];
(c) magnetic levitation [33].

The underlying principle behind these and other experimental techniques is to minimize the probability of heterogeneous nucleation through the following:

(i) an elimination of crucible induced nucleation;
(ii) separation of heterogeneous nucleants from the melt.

There is experimental evidence put forth in the published literature, which suggests that when these conditions are satisfied, the surface-induced nucleation processes are the primary limiting factor for the high undercooling extensions [34]. A schematic of the DE technique is shown in Fig. 2.

In this DE technique, fine droplets are formed by melting of a small amount of the alloy of interest in an inert carrier fluid (an inorganic salt being the most appropriate selection for the case of aluminum alloys) and stirring the immiscible fluids at a high rate. A large fraction of the fine droplets that form during stirring can be highly undercooled. It is also possible to promote a high degree of undercooling prior to solidification by using rapid heat extraction such as is present in (a) fine powder during atomization, and (b) on thin films during chill block melt spinning.

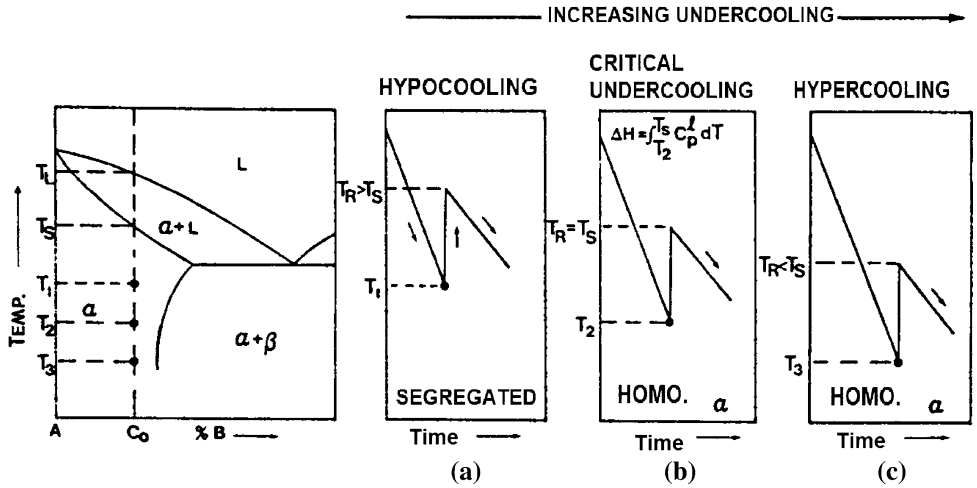

Fig. 1 Illustration of the concept of critical undercooling and hypercooling. The undercooling temperatures of alloy C_O are T_1, T_2, and T_3. T_R is the recalescence temperature [30]

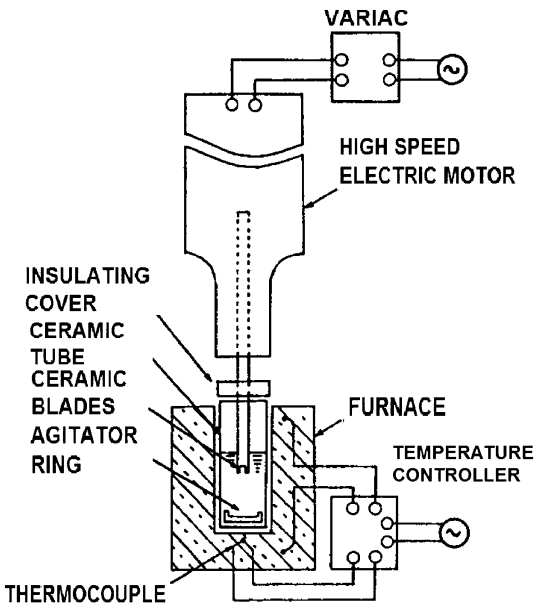

Fig. 2 A schematic diagram of the droplet emulsion apparatus [31]

Another economically viable approach to achieving rapid solidification, that is, imposing a high velocity of advance during continuous solidification, is accomplished by withdrawing a sufficiently thin specimen at high velocity (V) through a temperature gradient that is steep enough to constrain the solidification front from advancing the drawing velocity. When the solidification front is planar, its velocity [R] is defined as:

$$R = \mathrm{d}x/\mathrm{d}t. \tag{1}$$

The thermal gradient (G) is defined to be

$$G = \mathrm{d}T/\mathrm{d}x. \tag{2}$$

The product of planar solidification front velocity times the thermal gradient ($R \cdot G$) is defined as the cooling rate ($\mathrm{d}T/\mathrm{d}t$)

$$\mathrm{d}T/\mathrm{d}t = \mathrm{d}x/\mathrm{d}t \cdot \mathrm{d}T/\mathrm{d}x = R \cdot G. \tag{3}$$

A large value for G and R, or both, promotes a rapid growth of the solid phase. This facilitates in a refinement of the intrinsic microstructural features.

A third approach to achieving rapid solidification is by imposing a high-cooling rate during solidification, and is perhaps the most widely used. Besides the numerous experimental techniques available, the range of alloy compositions, which can be processed using this technique, is large. An important difference, between imposing a high-cooling rate during solidification and the two other approaches that are adopted and used, is that in the former approach the cooling is rapid prior to solidification, during solidification, and after solidification. This increases the probability of retaining the intrinsic microstructural and constitutional characteristics of the rapid solidification stage. The essential requirement of imposing a high-cooling rate during solidification is easily achieved by making one dimension of the solidifying volume very small, and subsequently exposing it to a rapid rate of heat extraction. A high rate of heat extraction effectively removes the thermal energy that is released (a) prior to solidification, (b) during solidification, and (c) following solidification. Since the nucleation and growth of the solid phases from the melt are closely linked with the evolution and dissipation of thermal energy, unusual structures tend to form under extreme, non-equilibrium conditions.

Rapid solidification techniques

In practice, there are a number of methods or ways that have been developed to produce the high rate of solidification (Fig. 3). A simple system of classification of the rapid solidification processes is to essentially divide them into those involving (Fig. 4):

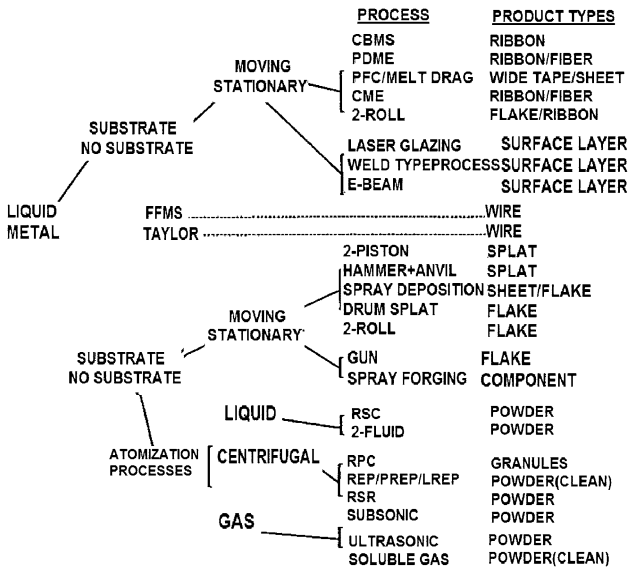

Fig. 3 Production routes for rapid solidification from the melt and their products [31]

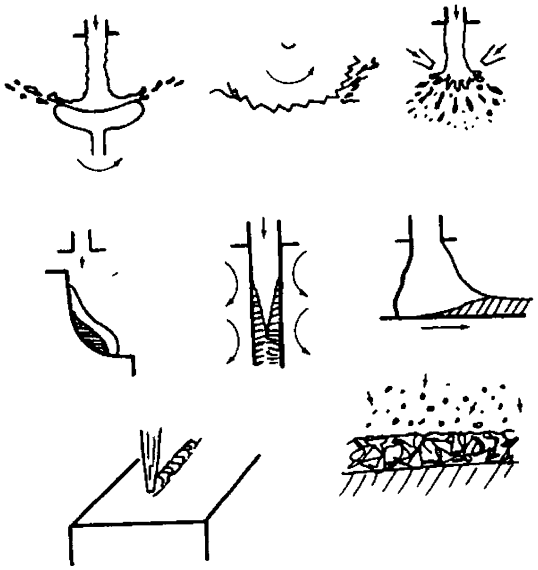

Fig. 4 A classification of the rapid solidification processes [35]

(a) the spray methods that involve fragmentation or atomization of a melt stream into droplets;
(b) casting of a melt stream (chill methods usually, but not always, involving stabilization rather than fragmentation of a melt stream);
(c) in situ melting and rapid solidification that takes place at the surface of the heat sink, which can be the same material as that being rapidly solidified.

Rapid solidification processing offers an avenue to circumvent some of the problems associated with conventional processing of metals and alloys and opens up new "pathways" for material development. The problems include but not limited to segregation at the macroscopic and microscopic levels, solidification shrinkage, microscopic cracking during solidification, and the tendency for 'local' heterogeneities in the microstructure.

The rapid solidification processes can be classified as a function of [35]:

(i) the resultant products (e.g., the powder production techniques);
(ii) the resulting microstructure (grain and particle size);
(iii) cooling rate generally measured by secondary dendrite arm spacing (SDAS).

A finer dendrite arm spacing (DAS) aids in minimizing shrinkage, the formation and presence of microscopic voids, and above all a more homogeneous microstructure at the microscopic level. A minimization of microscopic defects at the 'local' level is conducive for an overall improvement in mechanical properties of the finished product. A useful comparison of the SDAS versus solidification rate of different alloys is shown in Fig. 5 [36–38]. Superimposed on this figure are the other common processing techniques used, indicating the range in homogenization, which can be achieved for the different processes. The commercially viable techniques for RSP of metals and alloys are summarized in Table 1. A few of these techniques are shown in Fig. 6 [35]. Processes other than powder metallurgy (PM), which have also been used to produce rapidly solidified materials, include the following: (a) strip casting, (b) melt spinning, (c) laser spin atomization, (d) droplet quenching, and (e) gas atomization. The common products resulting from the use of such rapid solidification techniques include powders, flakes, ribbons,

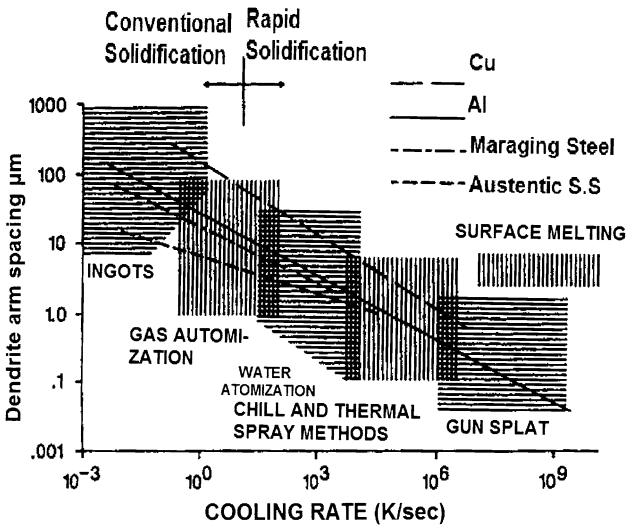

Fig. 5 Dependence of secondary dendrite arm spacing on the cooling rate for several alloys [38]

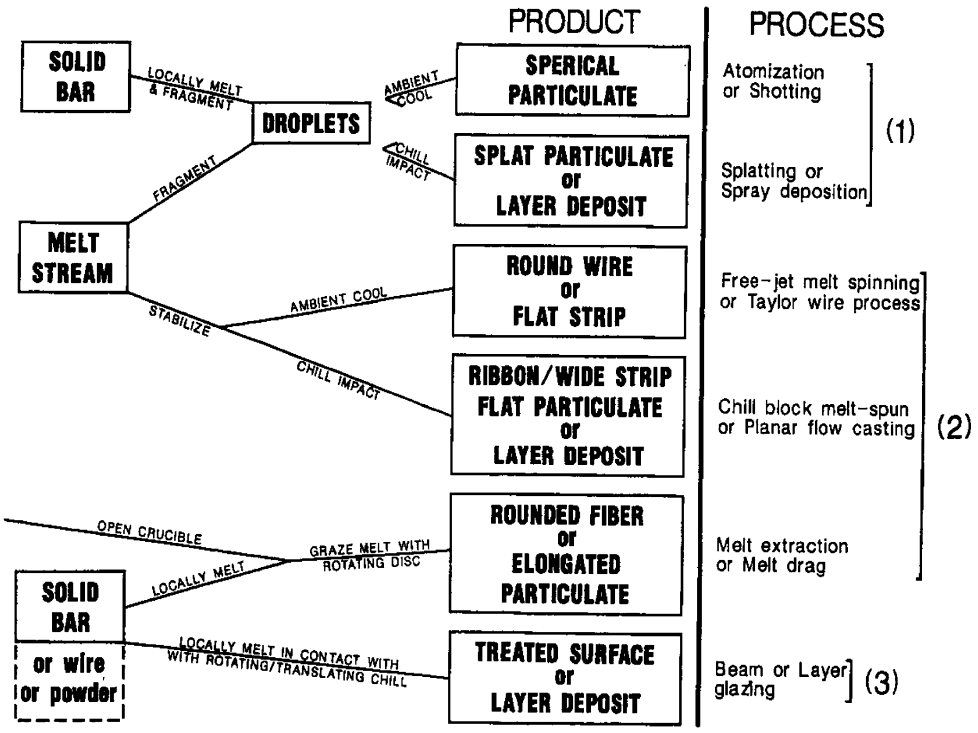

Fig. 6 The production routes for rapid solidification and rapid quenching from the available RSP methods: The key methods are (1) spray droplet, (2) continuous casting, and (3) melt in situ [35]

wires, and foils. An essential factor associated with all these RST is that the as-solidified product is very small (microns in size) in at least one dimension. This implies that the surface (s)-to-volume (v) ratio of the product is large. This is essential for obtaining an increased heat transfer coefficient while cooling from the liquid state to the solid state. The rapidly solidified particulates and/or strips, after quenching, require a post consolidation step to create reliable and useful engineering structures. Drop consolidation and spray forming are two viable techniques, which achieve sufficiently high cooling rates, thereby yielding the benefits of rapid solidification. However, in these two techniques, the latent heat of fusion and other process heat must be extracted in order to alleviate any post deposition effects.

Rapid solidification processing of metals and alloys

In this section, we discuss the three processes, which are most widely used for ferrous and non-ferrous based alloys. These are (i) atomization, (ii) ribbon or foil casting, and (iii) spray deposition.

Atomization

In atomization, a fine dispersion of droplets is formed when a high-energy fluid (gas or liquid) impacts the molten metal. Atomization occurs as a direct result of the transfer of kinetic energy from the atomizing fluid to the molten metal (Fig. 7) [39]. Although a fundamental understanding of the atomization process is yet to be established particularly in the case of molten metals, it is widely accepted that in most cases the droplets form from Rayleigh instabilities, which grow on the surface of torn molten ligaments (Fig. 8) [40, 41]. However, it is not necessary for the distribution of droplets formed initially to remain unchanged and a further breakdown can subsequently occur because of interactions with the atomizing gas. The droplets tend to undergo further changes as they are subjected to additional pressure forces and tend to experience disintegration when the dynamic pressure due to gas stream velocity exceeds the restoring force arising due to surface tension (Fig. 9). This condition is termed as the maximum stability criterion and is expressed as [40]:

$$0.5\rho g(\Delta V)^2 = C(\sigma_M/d_M), \tag{4}$$

where ρ is the density of the gas used, ΔV the velocity difference between the atomizing fluid and the molten metal, C an empirical constant whose value depends on the atomization system, σ_M the surface tension force, and d_M is diameter of the droplet.

The size distribution of the atomized droplets depends on the following:

(a) thermodynamic properties of the material, to include liquidus temperature, solidus temperature, melting

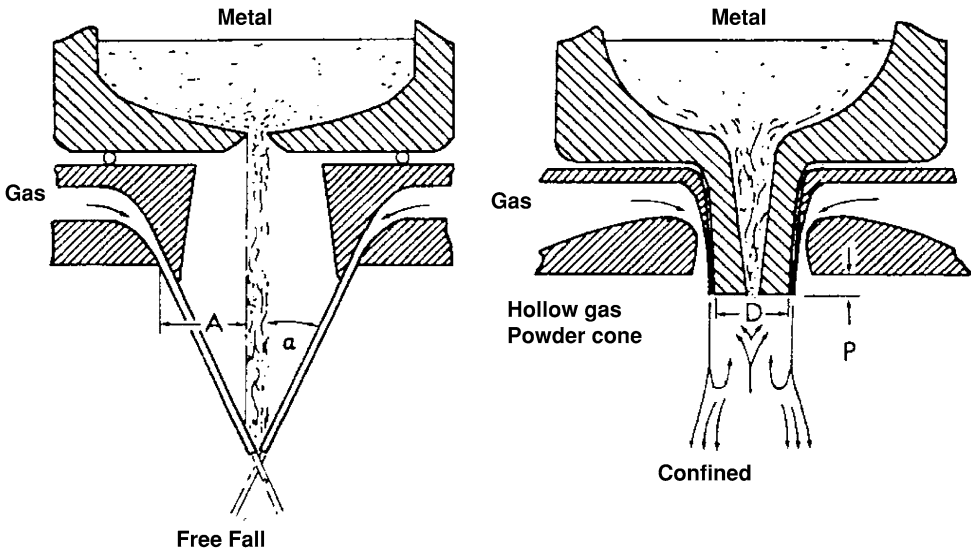

Fig. 7 The two fluid atomization designs. Alpha (α) denotes the angle formed by the free falling molten metal and the impinging gas. *A* The distance between the molten metal and the gas nozzle. *D* The diameter of the combined molten metal nozzle. *P* The overall protrusion length of the metal nozzle [39]

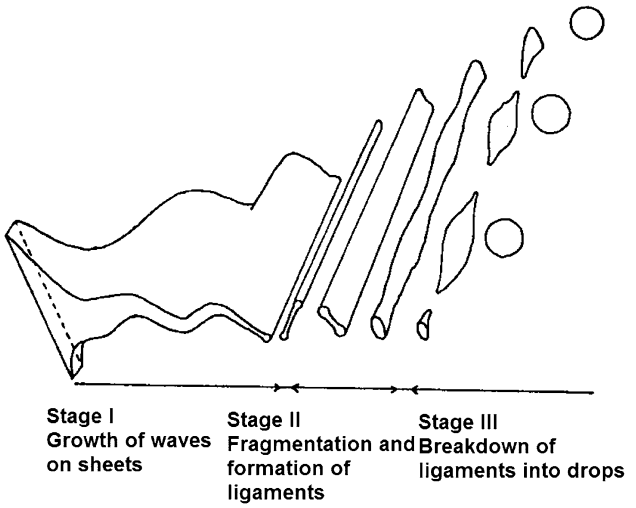

Fig. 8 A model for the disintegration of a liquid sheet by a high-velocity gas jet [41]

temperature, density, thermal conductivity, surface tension, heat capacity, and heat of fusion;

(b) the thermodynamic properties of the gas used, such as, density, heat capacity, viscosity, and thermal conductivity;

(c) the processing parameters, such as, atomization gas pressure, superheat temperature, and melt/gas flow ratio.

With specific reference to the processing parameters, it is found in the published literature that as the pressure of the atomizing gas increases, with all the other variables being kept constant, the mass median diameter decreases [42–48]. This is attributed to the conjoint and mutually interactive influences of: (i) an increase in the mass flow rate, and (ii) an increase in kinetic energy of the gas. Gas pressure has a complex effect on the atomization process. Gas pressure does affect the length of the supersonic core in the gas jets [45], while spreading of the gas jets leads to an increase in size of the powder particle [49]. The gas pressure during atomization has been reported to increase the metal flow rate by creating a low-pressure zone at the exit of the metal delivery tube that effectively aspirates the metal [50–53]. Thompson [54] reported an increase in the average powder particle size with an increase in gas pressure precisely due to this effect. Couper and Singer [50] developed a series of "flow pressure maps" to demonstrate that the metal flow rate could either be increased by aspiration (negative pressure) or retarded by bubbling (positive pressure). This phenomenon is affected both by gas pressure and by placement of the metal delivery tube.

A disintegration of the melt into droplets occurs almost instantaneously, by spheroidization of the individual droplets. This process is particularly rapid for molten metals because of their large surface tension forces (60–2,400 mJ/m^2) and low viscosities (0.602–6.92 m Pa s). The spherical or near spherical droplets continue to travel down the atomization vessel, rapidly loosing heat because of convection from the atomizing fluid. During flight, solidification is catalyzed heterogeneously in all but the smallest droplets because of one or a combination of the following: (a) bulk heterogeneous nucleation within the droplet, (b) surface oxidation processes, and (c) interparticle collisions. When the melt is subdivided into a large number of droplets, such as during atomization, the probability of achieving undercooling levels sufficiently high for homogeneous nucleation is inversely proportional to size of the droplet [31, 33, 34, 55]. The larger is the droplet, the chances of encountering heterogeneous nuclei increases. Since a large portion of the droplet population is comprised relatively of coarse sizes, an initial formation of

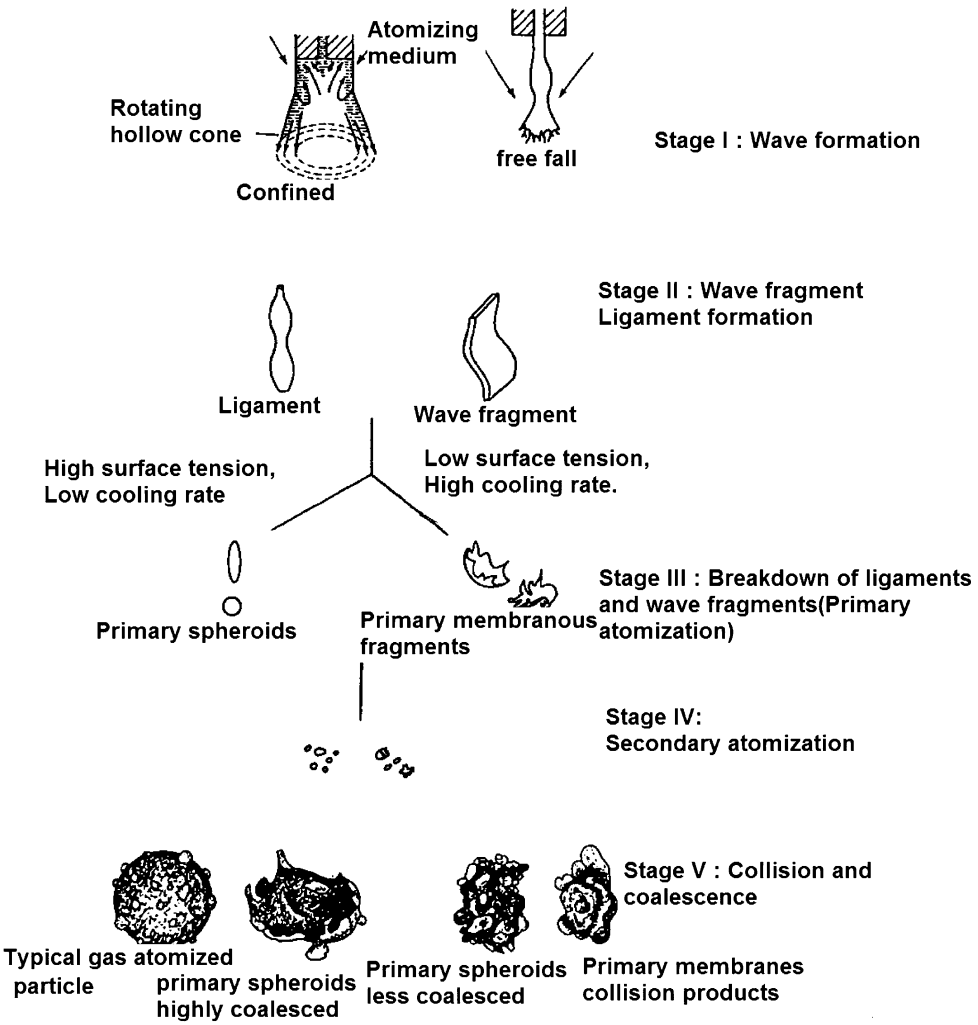

Fig. 9 Depiction of the particle configuration stages during atomization [35]

the solid phase occurs through mechanisms of heterogeneous nucleation.

The attainment of undercooling levels sufficiently large to promote homogeneous nucleation is nearly impossible because of the presence of heterogeneities in the melt such as: (a) inclusions, (b) un-dissolved phases, and (c) crucible debris. These heterogeneities effectively catalyze the solid phase. The use of catalysis decreases the possibility of achieving large undercooling that is required for homogeneous nucleation. The catalysts have been associated with surface oxidation processes, and their catalytic potency has been shown to depend on both size and chemistry [55, 56].

Another important phenomenon, which can effectively initiate solidification during flight, is interparticle collision. Interparticle collisions are highly probable because of the enormous turbulence that occurs within the atomization region. During the late 1980s, investigators [57] have used the phase Doppler interferometer to study the characteristics of both fluid flow field and particle flow field during atomization. Results of this study essentially revealed the following:

(a) the mass flux of particles in the atomization region to be high and spatially dependent;
(b) fluid flow to be extremely turbulent.

The energy provided by interparticle impact during turbulent fluid flow is likely to provide sufficient energy for the nucleation to be catalyzed. Thus, a viable way to promote microstructural homogeneity and minimize structural coarsening is to maintain a high-cooling rate (a) before solidification, (b) during solidification, and (c) after solidification. This is readily achieved during atomization, where fast interfacial growth velocities (ranging from 0.5 to 3.5 m/s), and resultant microstructural refinement, are maintained as a result of the conjoint and interactive influences of particles having a large surface-to-volume ratio, and an efficient convective heat flux to the atomizing gas (10^3–10^6 K/s) [30, 58, 59].

The degree of microstructural refinement achieved during solidification is often measured by the spacing of primary and secondary dendrite arms (DAS) [60]. For purposes of accuracy, the secondary arms are more commonly used for the purpose of spacing measurements, because they are generally more numerous and more regularly spaced when compared to the primary arms. In the presence of high cooling rates, the secondary arms are often prevented from growing, as occurs in cellular and degenerated dendritic solidification. The primary and secondary DAS are known to depend directly on product of the thermal gradient in the solidifying material and growth rate of the solid phase. The product has the units of cooling rate and the observed spacing is correlated with cooling rate or with solidification time [t_f].

During the decade of the 1980s, few investigators [61–64] have formulated and put forth models of the various heat transfer, solidification, and momentum phenomena during atomization. These models were utilized to predict the following: (i) droplet size distribution, (ii) droplet velocities, (iii) positions, (iv) temperatures, (v) cooling rates, and (vi) DAS, as a function of the processing condition. In these models, a computation of the droplet size distribution is accomplished by utilizing modifications to the original correlation proposed by Lubanska for predicting the variations in powder particle size with processing parameters [65]. Most of these models incorporate a number of assumptions, such as, (i) small Biot numbers, (ii) limited undercooling, or (iii) are based on simplistic thermal energy arguments, i.e., enthalpy formulation. The models can be used to provide a useful insight into the fundamental solidification phenomenon during atomization. Overall, the models provide an insight into the thermal and solidification behavior of the atomized droplets.

An example of results, which can be obtained from these models, is shown in Fig. 10 for an aluminum alloy droplet, which is 78 μm in diameter [63]. There are four well-defined temperature regions, which can be readily distinguished in this figure. The regions correspond to: (a) cooling of the liquid droplet, (b) recalescence, (c) cooling of the mushy droplet, and (d) cooling of fully solid particle. The four stages can be better appreciated in the cooling rate versus flight distance curve shown in Fig. 10b. In this study, the initial cooling rate experienced by the liquid droplets is of the order 2×10^5 °C/s. Such relatively high-cooling rates turn into heating rates, which reach up to about 4×10^6 °C/s, at which point recalescence takes place upon nucleation of the solid phase. The rise in temperature stops when the recalescence temperature is reached. When solidification is finally complete, the cooling rate rises again to about 1×10^5 °C/s. In net effect, the computed solidification behavior of the droplets is strongly dependent on the assumptions made in the calculation of

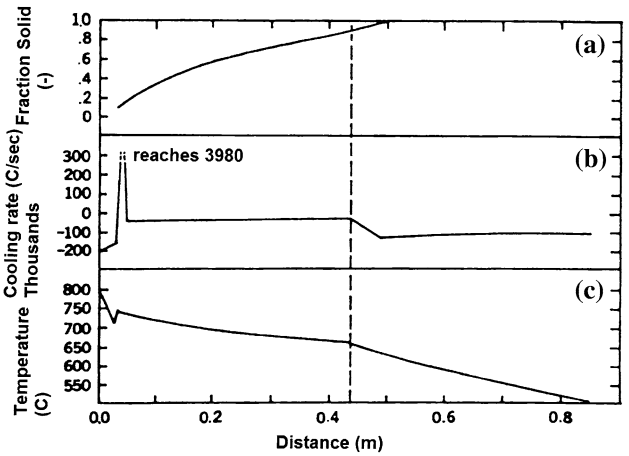

Fig. 10 Computed *a* fraction solid, *b* cooling rate, and *c* temperature, as a function of flight distance for a 78-μm aluminum droplet during spray atomization and deposition [63]

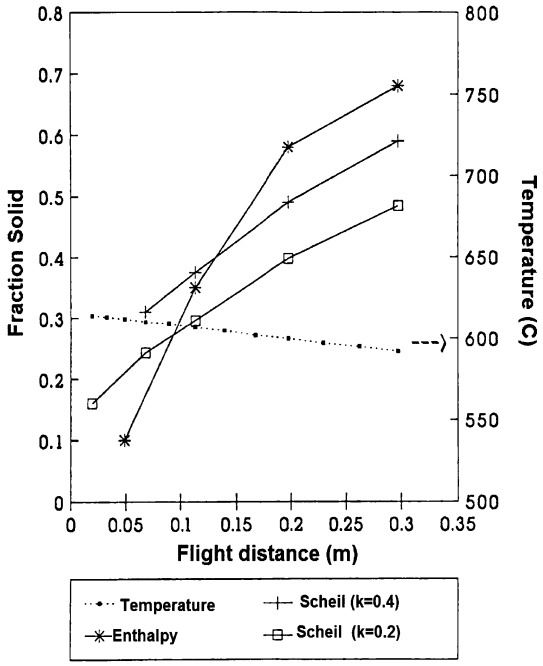

Fig. 11 A comparison of the prediction variation in fraction solid and temperature with flight distance using an enthalpy model and the Scheil equation [63]

the fraction solid (f_S) as a function of temperature. The variation in fraction solid (f_S) as a function of flight distance and temperature is shown in Fig. 11 (the enthalpy model) and compared with the results obtained using the Scheil equation [58]

$$f_S = 1 - [(T_m - T_L)/(T_m - T)]^{1/(1-k)}, \quad (5)$$

where k is the partition ratio, T_m the melting point of the pure metal, and T_L the liquidus temperature. The curves shown in the figure (Fig. 11) were calculated for two

values of the partition coefficient, i.e., $k = 0.2$ and $k = 0.4$, for the binary aluminum–copper alloy, where $k = C_S/C_L$, the ratio of solid composition to liquid composition.

The foil casting process

Progressive advancements in RSP can be directly traced to the interest aroused in the metallurgical community around the 1960s of the production of supersaturated solid solutions [1, 66], metastable solid solutions [1, 2], and amorphous phases [4] generated by Paul Duwez and his students using a new quenching device, which employed high-pressure shock wave of gas to propel a small droplet of melt against a chill plate. Splat quenching devices of this type produce quenching rates substantially higher than those generated by gas atomization, with cooling rates as high as 5×10^8 K/s being estimated for very thin portion of the splats [67]. There is a wide variety of splat quenching devices, most being similar in concept to the design of Duwez or to the piston and anvil apparatus constructed around the same time in Russia [68]. Experiments employing these devices did make substantial contributions to developing a more thorough understanding of the rapid solidification phenomena. Achieving rapid quenching by squirting a stream of melt onto the surface or edge of a flat wheel was known as chill block melt spinning, or simply as melt spinning [69, 70]. These processes were effective because when the molten metal stream is ejected onto a clean metal wheel in an atmosphere, which does but produce an undue degree of oxidation, the melt stream is dragged out into a thin strip, which adheres to the wheel as it solidifies. Subsequently, the thin strip separates from the wheel under the action or influence of stress produced by contraction of the solid metal strip as it cools.

The technique of melt spinning makes possible the production of long narrow ribbons, which, under favorable processing conditions, can cool at rates as high as 10^6 K/s. This process is widely used in rapid solidification studies: (i) because it is easy to execute, and (ii) because the quenching rates compare favorably to other available processes. However, it does have some limitations arising from the fact that the melt is squirted from a fine orifice. This geometry limited the ribbon width to about 3 mm, and generally results in even narrower ribbons when the highest quench rates are desired and achieved. Subsequent studies by few other researchers using the same technique resulted in the melt spun ribbons having a width that was 8–15 mm with ribbons having a width up to 25 mm for the brittle iron system. In general, a noticeable problem associated with using a small orifice, which is generally 1 mm or less in diameter, is that they are easily blocked by inclusions in the melt. These limitations resulted in the development of two techniques: (i) planar flow casting, and (ii) melt overflow process, which have the potential to yield large quantities of wide ribbon cooled at rates approaching 10^6 K/s. The advantages of planar flow casting over melt spinning are so great that various commercial enterprises have adapted the melt overflow process, which has many of the advantages of planar flow casting but is not patent protected. This process was eligible for patent protection considering that the basic patent was issued back in 1911 [71].

The solidification of metals by use of foil casting processes produces more rapid cooling than that experienced by all but the finest particles produced by gas atomization processes, so that refined structures are frequently formed, and metastable phases are often produced. As with gas atomization, the undercooling effects are important, and the rate of cooling slows during the course of solidification process. However, the higher rate of heat extraction during foil quenching makes these effects less important. Because of the regular geometry and steady-state nature of the foil casting process, considerable progress has been made in characterizing the parameters that govern the solidification phenomenon and microstructural development. A complete understanding and characterization of the solidification process during foil casting would require a determination of the time-dependent thermal profile through the thickness of the foil, and considerable understanding has been compiled and put forth in the open literature on this aspect [72–74].

The technology of rapid solidification has attracted a great deal of attention because of the wide range of opportunities it has offered materials science and engineering [75, 76]. The difficulties resulting from carrying out meaningful experimental measurements during RSP are well recognized [77]. Extreme temperatures, small sizes, and uncertain values of the material properties are some of the key issues that make measurements difficult. Therefore, an exclusive reliance on experimental results and observations has been an impediment to the development of new and improved processing techniques or methods. An approach that synergizes meaningful analysis and careful experiments is most likely to produce an insight that is essential for the successful implementation and effective execution of RSP systems. This insight is important for the development of optimal processes and improved control schemes.

A classification of rapid solidification processes

The variety of RSP techniques can be classified into four types. The basic criterion that governs this classification is based on the presence of common physical features among the different processes [77]. There is a single unifying

feature that is common to all rapid solidification processes. In order to obtain rapid solidification, a relatively thin molten layer must be brought into good thermal contact with a powerful heat sink. Although this feature is typical of RSP systems, it is quite adequate for an appropriate definition of the field. In an attempt to clarify the similarities and intrinsic differences among the various rapid solidification processes, a classification is appropriate and essential.

The traditional laboratory scale rapid solidification devices operate by producing only individual samples of the rapidly solidified material. During the initial years of research and development, processes of this type were classified as the single splat technique. However, it is also essential to consider the other processes in which fine particulate material is involved as members of the same group. This is often referred to as atomization processes. All of the processes in which the product is in the form of a long continuous ribbon or wire are grouped together as being continuous processes. A large number of the existing rapid solidification processes make efficient and effective use of the thermal conductivity of the bulk medium to produce rapid solidification. These processes are grouped together and termed as self-quenching methods.

The single splat process

In all of the single splat processes, a small mass of molten material is propelled against a cool chill. Upon impact with the chill surface, the melt spreads parallel to the chill surface and solidification initiates at the chill–melt interface. A schematic of this process is shown in Fig. 12. Since the fluid flow processes involved in spreading are at least an order of magnitude faster than the heat transfer rates, the splat thickness is dictated by spreading rate on the chill surface. By neglecting the time interval over which the spreading takes place, it is assumed that solidification starts once the splat has reached its final thickness. There exists a complex interplay between the underlying fluid dynamics involved in spreading and the local heat transfer processes that culminates in solidification.

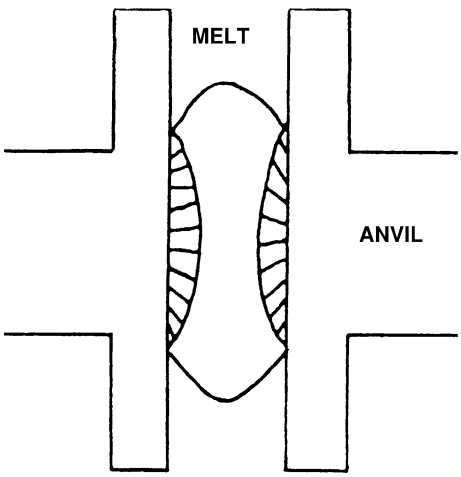

Fig. 12 Schematic representation of the single splat rapid solidification process [77]

The continuous process

The continuous processing technique is most convenient when large quantities of the product are required. In this technique, a small stream of molten material is directed against the surface of a rapidly moving chill. A schematic of the continuous RS process is shown in Fig. 13. During continuous processing, the melt spreads and solidifies as it impacts upon the substrate. By carefully controlling the process variables, it is possible to stabilize a small molten puddle at the point of impact of the metal stream with the chill surface so that a solidified product is extracted from inside the puddle. In the continuous process technique, the various processes operate on a bench mode, i.e., a small mass of material is poured at a time. The intrinsic mechanisms governing continuous RSP are rich and complex. At the starting level is the presence of a fluid dynamics problem of producing a stable molten jet of controlled dimension. Subsequently, the rate of spreading and meniscus formation on the moving chill have to be controlled by a complex interplay of fluid dynamics, capillary, and heat transfer phenomena [77].

The atomization process

In resorting to RSP by atomization, the primary objective is to destabilize a thin liquid film or jet and to concurrently produce a fine dispersion of droplets having good thermal contact with the heat sink (usually a cooler fluid). A schematic of this technique is as shown in Fig. 14. All of the atomization techniques start from a bulk shape (that is

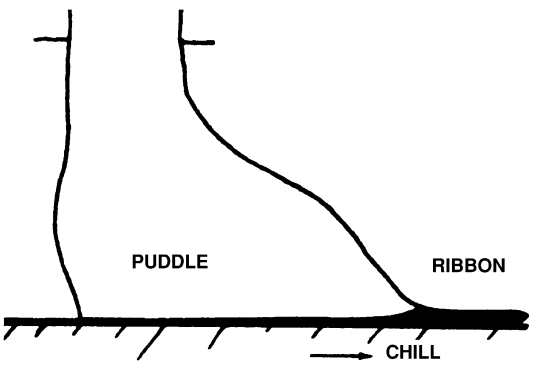

Fig. 13 Schematic representation of the continuous rapid solidification process [77]

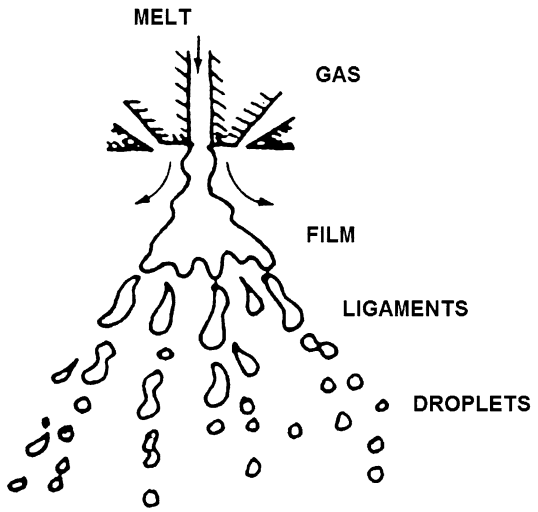

Fig. 14 A schematic representation of the atomization process

either molten or not) and terminate with a collection of fine particulates. This is the underlying feature of all atomization processes. Several mutually interactive physical processes take place during atomization. In the initial stages is the process by which small instabilities on the surface of the melt amplify until they are so catastrophic that droplet formation occurs. The powder size distribution is essentially non-linear and involves all of the peculiarities of a deforming fluid/fluid interface. The emerging spray of fine droplets is promptly intercepted by a cooler substrate. When this happens, the droplets collect as a bulk specimen by successively impacting on top of each other. In the period spanning the last three decades, i.e., since the early 1970s, there has been much interest in a modification of the basic atomization process since the product of processing is a form that should be closer to the final shape desired than a collection of powder in a simple atomization set-up. Such a process is termed as "spray forming" [78].

In order to obtain rapid solidification, a thin layer of melt having good thermal contact with a heat absorbing substrate is the necessary requirement. The effective result of this essential requirement is that rapidly solidified material is usually in the form of thin gage product (i.e., powder, ribbon, or foil). Since the initiation of the technology of rapid solidification, there has been an increased interest in the possibility of extending the benefits of rapid solidification for producing thicker sections. The spray form technique is a much sought after alternative. In this process, a fine spray of particulates produced by conventional liquid metal atomization process is intercepted in flight by a suitably designed collecting substrate. On impact with the substrate, the molten droplets in the spray form a splat and rapidly solidify. As additional droplets fall onto the previously solidified splats, a full-size deposit is eventually produced. When the operation is properly carried out, a fine equiaxed grain microstructure having relatively little micro-segregation is obtained. This highly desirable microstructure extends through the entire section of the deposit in clear contrast with the situation obtained in castings produced by methods that are more conventional. For developing a model, it is assumed that information is available on the thermal conditions of the spray as a function of distance from the atomization nozzle. This information is initially derived from a model of the liquid metal atomization process or alternatively obtained by actual experimental measurements in the atomization chamber. What is desirable and most essential is a calculation of the temperature and solidification rates in the growing preform both during deposition and after deposition.

The processes governing nucleation play a key role in the solidification of castings by controlling, to an extent, the initial structure, type, size scale, and spatial distribution of the second-phases. During many solidification processes, the size scale of the critical events governing nucleation are too small and the rate of their occurrence far too rapid to facilitate accurate observation using direct methods. The events governing nucleation in the solidification microstructure exerts a strong influence on grain size and morphology and overall compositional homogeneity. In large bulk castings, the solidification temperature corresponding to the onset of freezing is close to but slightly less than the melting point or equilibrium liquidus temperature. The offset of the solidification temperature with respect to the equilibrium temperature is referred to as undercooling or supercooling (ΔT). The level of melt undercooling at the onset of solidification is important to consider in developing an understanding of the variety of structural modifications and grain refining practices in common casting alloys and is the basis of recent solidification processing techniques using rapid solidification methods.

The self-quench processes

High-energy density pulses of short duration are used to melt shallow layers on the surface of bulk objects. The most commonly used energy sources in this case are the laser and electron beam gun. The energy is rapidly extracted from the molten layer by the underlying substrate and this results in the formation of a rapidly solidified surface layer. A schematic of this process is shown in Fig. 15. The high-energy density sources have been used by the electronics industry because of the high degree of control and the resulting narrow tolerances. By exercising a careful control on the energy input, it is possible to heat-treat the surface without melting it. This concept has been

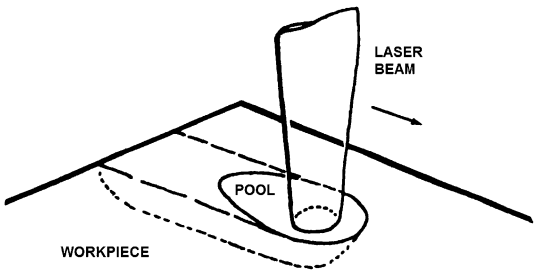

Fig. 15 A schematic representation of the self-quench process [77]

used for the manufacture of laser-hardened tracks in various grades of steel.

The phenomenon of nucleation during solidification

The occurrence of nucleation during solidification is a thermally activated process that involves a fluctuation growth in the sizes of clusters of the solid [80, 81]. Changes in size of the cluster are considered to occur by a single atom addition or by a removal exchange between the cluster and the surrounding undercooled liquid. For small sizes of the cluster, the energy involved in cluster formation reveals the interfacial energy to be the most dominant, since the ratio of surface area-to-volume of a spherical particle, having a radius 'r', is $3/r$. For the smallest sizes, the clusters are referred to as embryos. These are more likely to dissolve than grow into macroscopic crystals.

Homogeneous nucleation

For the case of homogeneous nucleation, the solid formation occurs without an involvement of any extraneous impurity atoms or other surface sites in contact with the melt. As a simplification, only the case of isotropic interfacial energy is considered. However, it is recognized that anisotropic behavior yields faceted shapes for the clusters. The energy involved in cluster formation for particles having a spherical geometry is expressed in terms of a surface energy contribution and volume energy contribution, as:

$$\Delta G(r) = 4\pi r^2\sigma + 4/3\pi r^3 \Delta G_V, \quad (6)$$

where $\Delta G(r)$ is the free energy change that is required to form a cluster of size r and $\Delta G_V = (\Delta H_f \cdot \Delta T)/(T_f \cdot V_M)$. In this equation, ΔG_V is volume free energy change, ΔT the degree of undercooling, T_f the equilibrium temperature in the furnace, ΔH_f the latent heat of solidification, and V_M the molar volume. For increasing values of undercooling, the critical radius of the nucleated particle (r_{cr}) is reduced ($r_{cr} \alpha \Delta T^{-1}$) and G_{cr} is reduced more rapidly (i.e., ΔG_{cr} α ΔT^{-2}). The cluster is considered to reach a stage of a nucleus capable of continued growth with a decreasing free energy when the critical radius (r_{cr}) is achieved. However, a stable growth of the nucleus occurs when the cluster size exceeds r_{cr}. The relationship between size of the cluster and number of atoms in a cluster (n_{cr}) is expressed as

$$n_{cr} V_a = 4/3\pi (r_{cr})^3/3, \quad (7)$$

where V_a is the atomic volume

Heterogeneous nucleation

Homogeneous nucleation is a difficult kinetic path for crystal formation because of the relatively large activation barriers for the development of a nucleus [80]. To overcome this barrier, classical theory predicts that large undercooling values are required. However, in practice, an undercooling of only a few degrees or less is the common observation with most castings. This behavior is accounted for by the operation of heterogeneous nucleation in which foreign bodies such as impurity inclusions, oxide films, and walls of the containing crucible promote crystallization by lowering the critical free energy required for nucleation. Since only a single nucleation event is required for the freezing of a liquid volume, the likelihood of finding a heterogeneous nucleation site in contact with the bulk liquid is appreciable.

In conventional metal casting crystal, growth and solidification are functions of atomic mobility. Both thermal and kinetic factors must be considered when determining whether crystal growth will be inhibited or accelerated. Whether spherical or needle-like in configuration, the metal particles tend to behave differently depending on their location within the composition, i.e., in the liquid, at the solid–liquid interface, or in the solid. While metals such as aluminum and copper have one crystal structure at all temperatures (face centered cubic), few other metals such as iron, cobalt, and titanium have different crystal structure at different temperatures (for example, iron is fcc at elevated temperatures and bcc at room temperature).

The heat released during solidification is large, approximately 270 MJ/ton or 116 Btu/lb for the conventional casting of steel. The higher the melting point of the metal, the larger is the latent heat of fusion. Therefore, solidification processing is governed by the nature of heat extraction from the cooling liquid. During cooling, most metals tend to shrink as they gradually solidify. The solidification shrinkage ranges from 3 to 8% for pure metals. The shrinkage results in the formation of microporosity, voids, and shrinkage cracking during solidification. A conjoint influence of all these intrinsic aspects does exert its influence on heterogeneous nucleation of crystals.

The thermal contraction of the solid that occurs during subsequent cooling tends to increase the risk of shrinkage if adequate care is not taken during casting of the metal [82].

The kinetics governing nucleation and crystal growth

An important yet difficult problem in the study of phase transitions and particularly those that take place during rapid solidification is an in-depth analysis of the first stages of the transformation. The new phase forms or initiates by a clustering or aggregation process that produces a definite distribution of nuclei having a variety of sizes. Some of the nuclei are large enough (called critical) that they can resist the destabilizing effects of the surface energy and can subsequently grow by incorporating additional molecules. Initially, the smaller nuclei decrease their free energy by re-dissolving in the parent (matrix) phase [83]. The presence of impurities and foreign substrates plays an important role in initiating nucleation. The presence of foreign substrates, by reducing the destabilizing influence of surface energy, allows the smaller clusters to become critical and initiate the growth process. In impure metals, little chemical driving force is essential to initiate the nucleation stage of the phase transformation. A necessary requirement for the occurrence of clustering is the existence of adequate supercooling in the melt to act as a driving force for the nucleation process. It is, therefore, required to determine the maximum degree of undercooling that a given melt can be subjected to. Physically, the melt must be supercooled to the point where homogeneous nucleation (i.e., nucleation in the absence of foreign matter) takes place or is initiated.

The formation of metallic glass

The problems related to nucleation and subsequent growth can be related to the process of formation of glass from a cooling melt. When the cooling rate imposed on the original melt is sufficiently high such that there is not enough time for the nucleation and growth processes to take place, the melt will not crystallize but the molecules will become more rigidly bound and eventually solidify without the formation of crystalline phases [84]. Researchers working on oxide glasses first established this phenomenon. However, it is the formation of metallic glasses by rapid solidification that attracted much attention to this technique [85]. The unexpected properties shown by metallic glasses led to an increased interest in the use of RSP [86].

Interface stability and solute redistribution

Upon the formation of a stable crystalline nucleus in a supercooled melt and concurrent growth of the crystal, another important problem surfaces. This relates to whether the moving solid–liquid interface will remain flat and stable or if it will develop morphological instabilities [17]. An understanding of this is important since it can be related to the microstructure developed in the solidified product. Even pure materials have the tendency to develop side-branching instabilities during solidification when the melt is rapidly undercooled [18, 19].

During RSP of alloys, the metastable supersaturated solid phases are frequently obtained [86]. The supersaturated phases result when the solidification rate is so large that there is not enough time for the occurrence of required solute partitioning that is commonly observed under conventional solidification conditions. The term solute, also known as “impurity trapping” [87], has been used to describe the redistribution phenomena resulting from rapid solidification. An analysis of solute segregation during directional solidification allows for the calculation of an instantaneous concentration field in the solid and liquid phases both during and after solidification [88]. A key assumption underlying these studies related to the solute redistribution problem is that of local equilibrium at the solid–liquid interface, that is, the equilibrium phase diagram gives the concentration of solute on both the liquid and solid sides of the interface. Although the existence of local equilibrium at the interface is appropriate for a wide range of cases in conventional solidification processing, the concept may not hold under rapid solidification conditions.

Early experimental observations of the solute-trapping phenomenon provided the desired incentive for a fresh look at the thermodynamics of solidification [89]. A careful consideration of the free energy-composition diagram for a binary system reveals that solid phases having a wide range of solute content can be produced from the melt of a given composition. Further, a solid with a maximum amount of the solute can be produced by rapid solidification of a liquid with composition given by the intersection of the free energy curves of the solid and liquid phases in the phase diagram.

Early estimates of the solute redistribution during rapid solidification were obtained from a simple model of understanding the solidification kinetics of an undercooled binary alloy melt [90]. This simple model essentially relies on an assumption of equilibrium at the “local” level for part of the calculation. The early model provided one of the first quantitative explanations for the occurrence of solute trapping in metal-based alloys. In this model, the solidification process is considered to take place in three distinct stages [90].

(a) Freezing initiates in the undercooled melt with complete trapping of the solute. As a direct result of

the rapid freezing, the sample temperature rises from the nucleation value to the solidus.

(b) Recalescence continues past the solidus temperature until the sample reaches the maximum recalescence temperature (say T_R). Under these conditions, the concentration of solute at the interface is estimated from the phase diagram of the metal or alloy.

(c) The sample gradually cools down to room temperature and solute redistribution is estimated using simple laws governing the Scheil equation.

Rapid solidification processing of constituents of a composite materials

The RSP methods, currently utilized for the manufacture of advanced metallic, intermetallic, and the emerging generation of discontinuously reinforced metal-based composites, are grouped according to the temperature of the metal during processing. Accordingly, the processes are classified into the categories of:

(a) solid phases processes;
(b) liquid phase processes;
(c) two-phase (solid/liquid) processes.

The solid phase processes

The fabrication of reinforced metal matrices, particularly particulate reinforced, from bonded elemental powder involves a number of stages prior to final consolidation. The salient attributes of three key processes, i.e., (i) PM processing, (ii) high-energy rate processing, and (iii) dynamic powder compaction are presented.

Powder metallurgy processing

Solid phase processes essentially involve a thorough blending of powders of the rapidly solidified alloy with the reinforcing phase, i.e., fine particulates, platelets or whiskers, through a series of steps. The sequence of steps includes the following:

(a) sieving of the rapidly solidified particles;
(b) precision blending of the reinforcement, i.e., whiskers or particulates, with the powdered alloy matrix;
(c) compressing the reinforcing phase and metal powder mixture to approximately 75 percent density;
(d) the metal or intermetallic powder-reinforcement mixture is then loaded into a die, heated and subsequently degassed to remove absorbed and adsorbed gases prior to consolidation to get a billet;
(e) the billet is cooled, homogenized and scalped prior to extrusion, forging, rolling, or drawing.

Secondary fabrication of the composite billet normally involved all other applied metal working practices [91–94]. A flow chart that depicts the process sequence, used at the former Advanced Composite Materials Corporation (ACMS, Greer, South Carolina, USA), for the manufacture of PM, discontinuously reinforced aluminum alloy composites [DRA MMCs] is shown in Fig. 16. With time, this technology has been extended and developed to various degrees of commercial success by few other manufacturers.

An important step in the manufacturing sequence of discontinuously reinforced metal matrices involves a proper selection of the discontinuous reinforcement and the matrix alloy. The key criteria for the selection of a reinforcement phase includes the following [95]: elastic modulus, tensile strength, density, melting temperature, thermal stability, compatibility with the metal–matrix, thermal coefficient of expansion, size and shape, and cost. The most widely chosen and used metal matrices and ceramic reinforcements for the synthesis of metal–matrix composites (MMCs) are summarized in Table 2. The properties of the reinforcement are summarized in Table 3.

In the PM approach developed by the Aluminum Company of America (ALCOA), the reinforcement material is blended with rapidly solidified powders. The blend is then consolidated into billets by cold compaction,

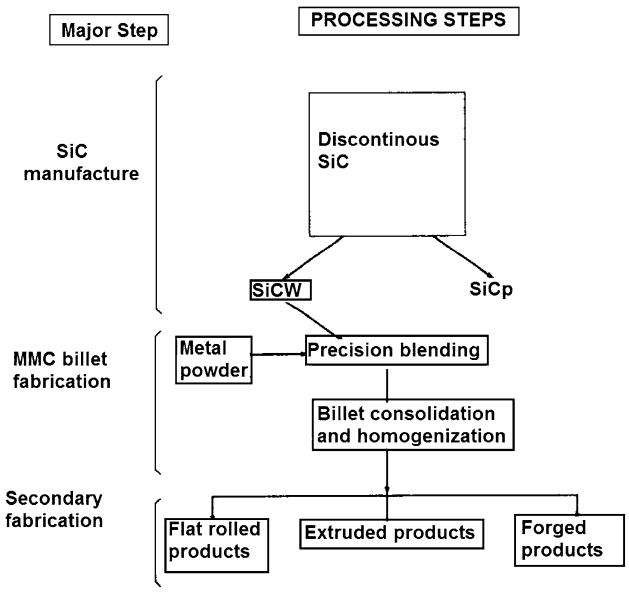

Fig. 16 Flow chart showing the key fabrication steps for a discontinuously reinforced silicon carbide metal–matrix composite at the ACM Corporation [96]

Table 2 Metal–matrix composites key matrices and reinforcements [91, 95]

Matrices	Reinforcements
Aluminum	Continuous fibers
	Boron(coated and uncoated)
	Silicon carbide
	Alumina
	Graphite
Magnesium	Wires
	Tungsten
Titanium	Discontinuous fibers
	Alumina
	Alumina-silica
	Graphite (chopped)
Copper	Whiskers
	Silicon carbide
Superalloys	Particles
	Silicon carbide
	Boron carbide
	Alumina
	Titanium boride

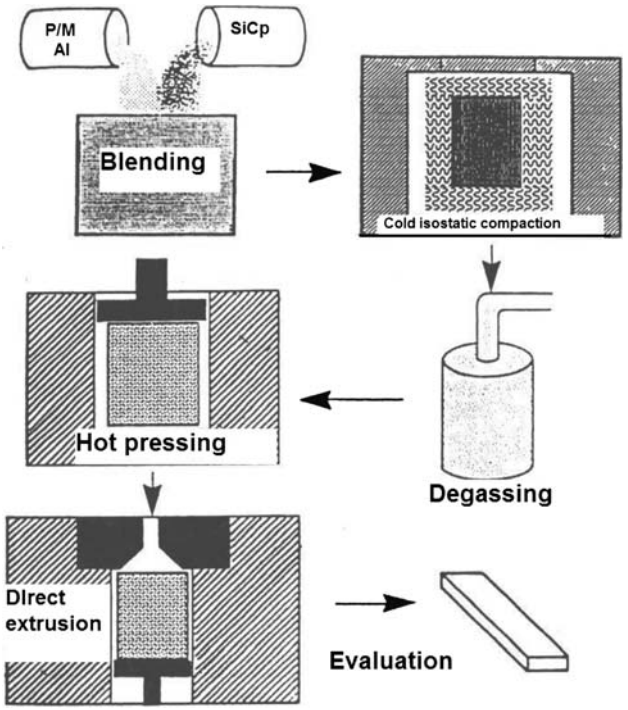

Fig. 17 Schematic of the process used at the Aluminum Company of America for an aluminum alloy-silicon carbide particulate composite [97]

Table 3 Properties of selected ceramic reinforcements [95]

Ceramic	Coefficient of expansion (10^{-6}/°F)	Strength (MPa)	Elastic modulus (GPa)
BeO	4.1	24 (2000 °F)	190 (2000 °F)
MgO	6.45	41 (2000 °F)	150 (2000 °F)
ThO_2	5.3	190 (2000 °F)	200 (2000 °F)
UO_2	5.3	–	175 (2000 °F)
ZrO_2	6.67	85 (2000 °F)	130 (2000 °F)
CeO_2	6.9	600 (75 °F)	200 (75 °F)
Al_2O_3	4.4	220 (2000 °F)	380 (2000 °F)
$TaSi_2$	6.0	–	340 (2000 °F)
$MoSi_2$	4.85	280 (2000 °F)	280 (2000 °F)
WSi_2	5.0	–	250 (2000 °F)
TiB_2	4.6	–	410 (2000 °F)
ZrB_2	4.5	–	503 (75 °F)
TiC	4.22	55 (2000 °F)	270 (75 °F)
ZrC	3.7	90 (2000 °F)	360 (75 °F)
HfC	3.7	–	320 (75 °F)
VC	3.98	–	430 (75 °F)
NbC	3.8	–	340 (75 °F)
TaC	3.59	–	360 (75 °F)
Mo_2C	3.23	–	230 (75 °F)
WC	2.83	–	670 (75 °F)
B_4C	3.38	2800 (75 °F)	450 (75 °F)
SiC	3.00	–	325 (2000 °F)
AlN	2.69	2100 (75 °F)	310 (2000 °F)

outgassed and subsequently either hot isostatic or vacuum hot pressed (Fig. 17) to form billets for subsequent fabrication [96]. The cold compaction density is controlled in order to maintain an open, interconnecting porosity. This is essential during the following stage of degassing, or outgassing, during the pressing operation. The process of outgassing involves the removal of: (a) the adsorbed gases, (b) chemically combined water, and (c) other volatile species, through the synergistic action of heat, vacuum, and inert gas flushing [96]. An advantage of the PM technique is an ability to use the improved properties of rapidly solidified powder technology for the manufacture of MMCs [95].

In the process developed by the Advanced Composite Materials Corporation (ACMC) to make, discontinuously reinforced metal–matrix composites (DRMMCs), the atomized metal powders, and the reinforcing particulates are mixed using proprietary techniques. A careful control of the processes is critical for the production of homogeneous, high performance composite materials. The metal powder–reinforcement particulate mixture is then loaded into a die, degassed, and subsequently vacuum hot pressed at a temperature above the solidus temperature of the matrix alloy. The presence of molten metal during hot pressing allows for a full densification of the billet at moderate pressure, even when small high surface area reinforcements are used [97].

The high-energy rate processes

An approach that has been successfully utilized to consolidate rapidly quenched powders containing a fine dispersion or distribution of ceramic particulates is known as the high-energy rate processing [98, 99]. In this technique, the consolidation of the metal–ceramic mixture is achieved using high energy and at high rates from a homopolar generator. The homopolar generator converts the stored rotational kinetic energy into electrical energy using the Faraday effect. In this particular process, the degassed powder is subjected to a pulsed high current discharge under low pressure. The current pulse is high, reaching a maximum of 1.0 MA after 200 ms and lasting for about 1–2 s. At the onset of the pulse, pressure is stepped up with the primary objective of ensuring electrical conductivity to the powder mixture and to concurrently aid in smooth and easy consolidation of the powder mixture by applying a mild forging. The high-current pulse is transmitted between two rams that are driven by a hydraulic press. A pair of floating plungers made from copper then compresses the metal–ceramic powder (reinforcement) mixture. The copper plungers serve as an effective heat sink to accelerate rapid cooling of the consolidated powder by conduction [99]. The ultimate bonding, which occurs during consolidation, results from the pulse resistive heating that is produced at the inter-particle surfaces. The hot and rapidly applied thermal cycle facilitates in consolidation of the powder mixture, without the occurrence of coarsening, when compared one-to-one with the conventional consolidation techniques. The high-energy high-rate consolidation process does produce metal-based composites having densities greater than 95% of the theoretical density.

Dynamic powder compaction

Refined and at times required metastable microstructures, in metal-based and intermetallic-based systems, can be obtained by the use of rapid solidification techniques. The consolidation step in the process involves prolonged thermal exposure with a resultant coarsening of the fine microstructural features. A method, which safely avoids such thermal excursions and concomitant microstructural changes, is dynamic powder compaction (DPC) [100, 101]. The dynamic compaction and static compaction processes differ in the following [102–104]:

(i) the speed at which the compaction process occurs;
(ii) the physical mechanisms taking place at the very microscopic level.

In the static compaction process, a relatively uniform pressure is applied and either concurrently or subsequently a high temperature is imposed to initiate and bring about long-range diffusion. This is essential for the following reasons:

(a) causing and promoting particle bonding while concurrently either eliminating or minimizing porosity;
(b) to enable the metastable material to decompose.

The dynamic compaction occurs by the passing of an intense shock wave from one side of the material to the other side while being compacted. Very high pressures are produced and the resultant densities facilitate little or no requirement for the occurrence of long-range diffusion. Further, the occurrence of localized shearing between the particles results in excessive heating of the surface. This facilitates in promoting and enhancing an effective bonding between the powder particles. The dynamic powder compaction technique is useful for the purpose of compaction of thermally unstable materials. This technique is rapidly growing and commercially viable since it offers the potential for exploiting all of the benefits of rapid solidification technology [105–107].

Consolidation processes

Clearly, the rapidly solidified particulates must normally be consolidated into fully dense bodies before they can be of any commercial interest. The consolidation sequence for rapidly solidified PM particulates essentially consists of the following (i) cold pressing, (ii) degassing, and (iii) hot consolidation, followed by (iv) hot working step (see Table 4). The degassing step is performed after the powder has been consolidated to approximately 75% density. This allows for an effective evacuation of the volatile species in the powder. In general, the processes for consolidation and densification are grouped together as follows [108–113].

1. Forging and rolling: in order to be able to handle the end-product, these methods require the preparation of a preform either by hot mechanical pressing, cold pressing, and sintering, or some other practical means.
2. Hot isostatic pressing (HIPing): involves placing the powder in a container that plastically deforms at the consolidation temperature. The powder is then brought up to temperature with subsequent compression under a high-pressure fluid (usually argon). This results in a fully dense piece, but the presence of oxide particles at the prior particle boundaries does severely limit the utility of this process to aluminum alloys.
3. Pseudo-hip processes: because of the high costs and long cycle times associated with conventional HIPing, a number of pseudo-HIP processes have emerged [114]. In particular, the STAMP process produces a

Table 4 Powder metallurgy process for aluminum–iron–cerium powder alloys [113]

Number	Step	Remarks
1	Alloy powder	Atomized and screened to −200 mesh size
2	Compact	Alloy powder cold isostatically pressed (CIP) to 75% dense compacts
3	Encapsulate	Each compact encapsulated in an aluminum container having an evacuation tube on one end
4	Degas	The canned compact is evacuated at an elevated temperature under dynamic vacuum and then is sealed
5	Hot press (HP)	The degassed compact preheated to an elevated temperature not higher than the degassing temperature is pressed into a fully dense billet in a blind die using extrusion process
6	Scalp	The vacuum hot pressed (VHP ed)[a] billet is machined into the extrusion billet while removing the aluminum can
7	Hot work	The VHP billet preheated to an elevated temperature is extruded at a medium extrusion ratio or, for subsequent rolling or forging, at a low extrusion ratio

[a] Degassing and hot pressing are often called, as a combined process, vacuum hot pressing (VHP)

billet that must be either forged or rolled into the final part. The STAMP and CERACON processes make use of large forging presses to achieve densification. However, the crucible ceramic mold process makes use of conventional HIP equipment. The CERACON process is shown in Fig. 18. In order to compact the Al–Mg–Si alloy 6061, the powder is cold pressed into pellets prior to consolidation. The pellets are preheated to about 630 °C for 9 min, and then embedded in a pressure transmitting medium [PTM] (ceramic or graphite), which fills the preheated die. A large pressure is applied in a time span of few seconds using a computer controlled ram [115].

4. Hot extrusions and other hot working processes: the powders are packed into containers, sealed, evacuated, and then hot extruded.

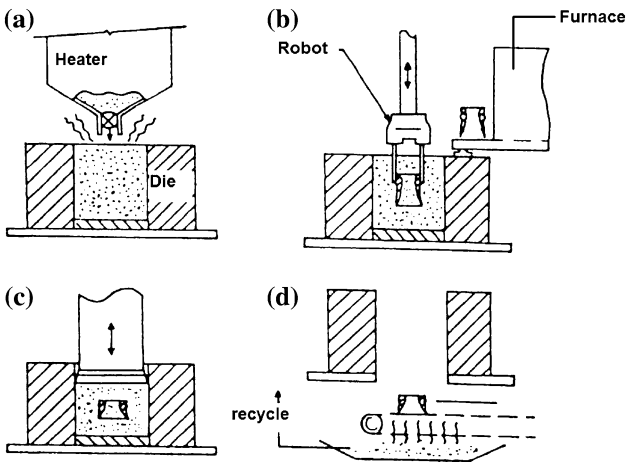

Fig. 18 A schematic of the CERACON process. **a** The preform and the pressure transmitting media (PTM) are heated, the hot PTM is then placed inside the die. **b** A robot immerses the preform into the PTM. The transfer of PTM aluminum is carried out in ambient air. **c** The die is transferred to an uniaxial press, which consolidates the Preform into a fully dense part. **d** After pressing, the part is removed from the die and the PTM is recycled [115]

5. Dynamic consolidation methods, such as explosive and other high-energy rate processes: these employ high pressures produced by the impact of fast moving punches or shock waves to (i) cause densification of the particulates, and (ii) promote interparticle bonding [116–119]. During dynamic compaction, the presence of large amount of energy at the powder particle contact points is conducive for the initiation of surface melting and inter-particle bonding.

Each of these approaches has some noticeable disadvantages, but all have been utilized to varying degree to produce materials having an attractive combination of properties. The particular process, which has been most widely used and for which the largest database is available is hot extrusion. The salient advantages of the hot extrusion process lie in its ability to provide large amounts of mechanical working while concurrently yielding a fully dense product. During the extrusion process, large hydrostatic compressive forces coupled with a normal force component make the preform flow through a die. The shear component that results form frictional forces in the deforming metal takes up one-half of the total energy required for extrusion. The extrusion process provides far more plastic deformation than any other single metal working step [110, 114].

The three basic methods most commonly used for the extrusion of metal powders are [114]:

(a) filling the extrusion container with loose metal powder and then extruding;
(b) cold or hot pressing coupled with sintering the powder immediately followed by extrusion;
(c) cold pressing in a can followed by extrusion of both the can and powder.

When using the first two methods, alloys sensitive to oxidation (i.e., aluminum alloys) must be processed in an inert environment. If not, the interconnected porosity

present on the surface will facilitate in promoting internal oxidation of the part. Machining the "can" subsequent to processing does result in a direct increase in cost when using the extrusion process.

The technology and advances in spray processing

Using the basic principles of rapid solidification, a variety of processing techniques have developed and emerged as attractive and commercially viable alternatives to optimize both the microstructure and properties of monolithic metals and their alloy counterparts and even metal and/or intermetallic matrices reinforced with ceramic particulates, i.e., composite materials. Of the several techniques that have been developed and implemented during the recent decade, the technique of spray processing offers an opportunity to synergistically utilize the benefits associated with fine particulate technology. A few of the notable benefits include: (a) refinements in intrinsic microstructural features, (b) modifications in alloy chemistry, (c) improved microstructural homogeneity, (d) in situ processes and, in a few cases, (e) near-net shape manufacturing. In the time spanning the last two decades, the technique based on principles of spray technology has rapidly evolved, and there presently exists a variety of spray-based methods. These include the following:

(a) spray atomization and deposition processing [120–137];
(b) low-pressure plasma deposition [138–140];
(c) modified gas welding technique [141];
(d) high-velocity oxyfuel (HVOF) thermal spraying [142, 143].

For the case of composite materials, the technique of spray processing involves a thorough mixing of the discontinuous reinforcements with the matrix material under conditions of non-equilibrium.

In this section, we provide a detailed overview of the technique of spray atomization and deposition processing and a succinct overview of the techniques of low-pressure plasma deposition, modified gas welding, and HVOF thermal spraying.

Spray atomization and deposition processing

Commercialization of the technique of RSP has been limited due to difficulties associated with the production of bulk shapes. These problems resulted from the presence of oxides on the reinforcing particulates. In an effort to control the volume fraction of oxide particles present in the consolidated rapidly solidified alloy obtained by the PM technique, and to concurrently simplify the overall processing, the technique of spray atomization and deposition processing emerged. During the last three decades, i.e., since the early 1980s, this processing technique has been the subject of increased research activity.

A. Singer at the University College of Swansea, United Kingdom pioneered the basic principles of spray deposition during the 1970s. Singer proposed the production of rolled strip directly from molten metal as an attractive and economic alternative to the conventional practice of casting and rolling of large ingots [144, 145]. Singer examined and studied the spray rolling of metals as an alternative to the process initially developed at the Reynolds Metal Company in 1967 [146]. In this process, an aluminum alloy was centrifugally atomized, reheated, fed into roll gaps, and subsequently hot rolled to produce strips in a continuous operation [147]. The general principle of spray atomization and deposition is to atomize a stream of molten metal using high-velocity inert gases, such as argon or nitrogen, and to direct the resulting spray of molten metal onto a shaped collector, which can be either a mold or a substrate. On impact with the substrate, the very fine particles in the molten metal stream flatten and weld together to form a hot, high-density preform, which is conducive for being readily forged to form a fully dense product. The surface of the substrate must be prepared in such a way that the first layer of atomized droplets will adhere onto it to form a smooth quenched layer. Singer performed his studies on aluminum alloys [144, 145]. The atomized droplets were approximately 100–150 μm in diameter, and were produced by using conventional atomization equipment.

Subsequent to this development, Osprey Metals Ltd (Neath, South Wales) implemented the early ideas of Singer for the production of forging preforms. This effort was undertaken as a direct result of the increasing pressure imposed on the metal-forming industry to (a) reduce manufacturing costs, (b) improve material utilization, (c) improve material structure and properties, and (d) enhance efficiency [147–151].

The OSPREY^{TM} deposition process

The enhanced interest and resultant development and emergence of the Osprey^{TM} process as a commercially viable and applicable technique was attributed to several mutually interactive factors, the most important of which being "flexibility." The Osprey ^{TM} process technique incorporates the salient advantages of PM processing without involving the disadvantages associated with consolidation. The advantages of this technique are manifold and include the following [151–153]:

(1) the rapid formation of a range of semi-finished products such as tubes, billets, and strips directly from the melt;
(2) creation of composite materials, which can contain up to and over 20 volume percent of the reinforcement by an injection of the particulates into the atomized stream of the molten alloy;
(3) the processing of "difficult to work" conventional alloys and novel alloy compositions as a consequence of rapid solidification;
(4) potential for the economic manufacture of a spectrum of products as a direct consequence of the high rates of metal deposition that are available coupled with the concurrent elimination of several of the processing steps required in ingot metallurgy and PM techniques;
(5) facilitates secondary processing routes without prolonged soaking times and/or the large deformation ratios required for fine grain size, segregation-free microstructures.

The noteworthy advantages of the Osprey™ deposition technique compared with other closed-nozzle, rapid solidification processes include the following:

(a) use of inert gas environment avoids oxidation of the droplets;
(b) large melts can be easily handled without nozzle erosion problems;
(c) the gas/metal ratio and gas pressure can be adjusted to suit both novel and new alloy compositions;
(d) it is possible to control the direct impingement of the molten, semi-molten and atomized particles on the surface of a collector, thereby ensuring full density products having novel microstructures.

The key stages in the Osprey™ technique are (i) melting and dispensing, (ii) gas atomization, deposition, and (iii) collector manipulation. The melting is undertaken by induction heating in a furnace, which is directly linked with a tundish. The molten metal then flows from the tundish into the gas atomizer. The melting and dispensing operation is carried out in a vacuum chamber

Production of metal-based (MMCs) and intermetallic-based (IMCs) matrix composites is accomplished by injecting the reinforcing ceramic particulates into the atomized stream of molten metal leading to co-deposition with the atomized metal or intermetallic onto the substrate. A careful control of the atomizing conditions and particulate feeding conditions is both required and essential in order to facilitate a near homogeneous distribution of the reinforcing ceramic particulates in the microstructure [154, 155]. The primary attraction of this technique is the rapid production of semi-finished composite products in a combined atomizing, particulate injection and deposition operation. Further, this method offers notable cost savings compared to the other RSP techniques for the manufacture of both metal–matrix based and intermetallic-based composite materials.

During the early years, the Osprey™ process has produced ranges of conventional aluminum alloys containing silicon carbide (SiC) particulate. These include both the wrought alloys [2000 series (Al–Cu–Mg), 6000 series (Al–Mg–Si) and the 7000 series (Al–Zn–Mg)] and the cast aluminum alloys [(Al–Si)] [156]. The versatility of the technique has been demonstrated by an ability to spray diverse metal matrices such as commercially pure aluminum and the emerging generation of aluminum–lithium based alloys. The final quality of the aluminum alloy-based MMCs are critically dependent on composition of the matrix alloy.

The salient advantages of the spray atomization and deposition process is that it inherently avoids the extreme thermal excursions, and the resultant degradation of mechanical and interfacial properties and extensive macrosegregation, normally associated with conventional casting processes. Furthermore, this approach eliminates the need to handle fine reactive particulates as is necessary with conventional PM processing. A series of studies based on spray atomization and collection processes but using high-pressure gas atomization for the spraying of fine, rapidly quenched droplets, in a controlled atmosphere, resulted in the development and emergence of the technique of Variable co-deposition of multiphase materials (referred to henceforth as VCM) [120, 121, 157].

The variable co-deposition of multiphase materials (VCM)

In the variable co-deposition of materials (VCM) process, the matrix material is disintegrated into a fine dispersion of droplets using high-velocity inert gas jets (Fig. 19). Simultaneously, one or more jets of the strengthening phase(s) are injected into the atomized spray at a prescribed spatial location (Fig. 20). Good interfacial control is achieved by injecting the reinforcing ceramic particulates at a spatial location where the atomized spray of the metal contains only a limited amount of volume fraction of liquid. By this, the contact time and thermal exposure of the reinforcing ceramic particulates with the partially solidified matrix are minimized and interfacial reactions are closely controlled. Further, a tight control of the environment during processing minimizes oxidation and other environmental effects [120, 121, 157, 158]. For situations where reactivity between the matrix material and the reinforcement is negligible, the reinforcing phases are safely introduced into the liquid alloy prior to the initiation of spray deposition [159].

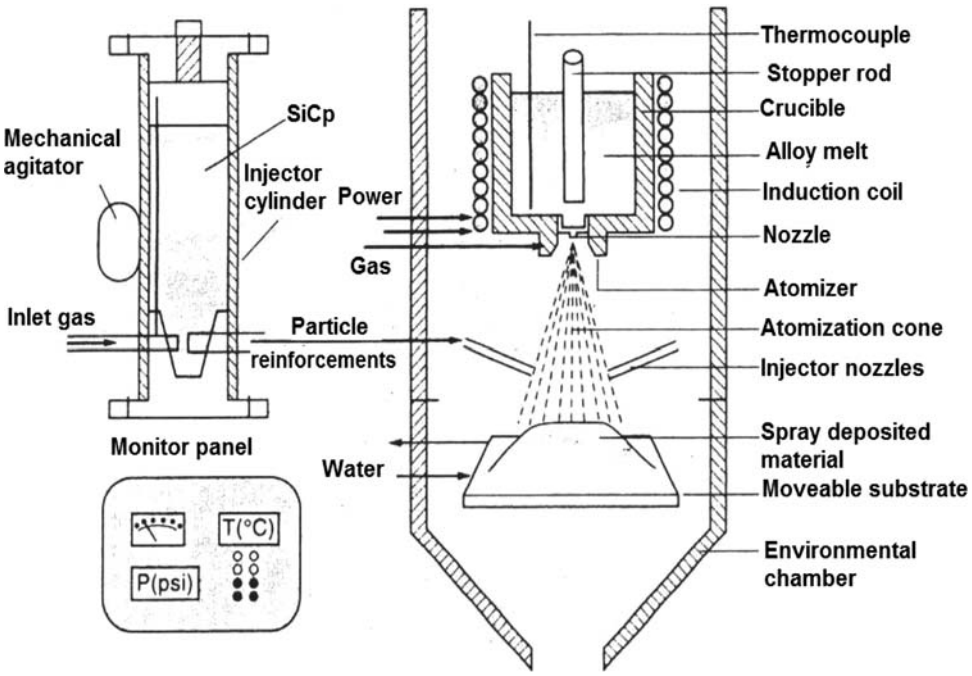

Fig. 19 A schematic showing the experimental arrangement for controlled spray atomization and deposition processing [118, 121]

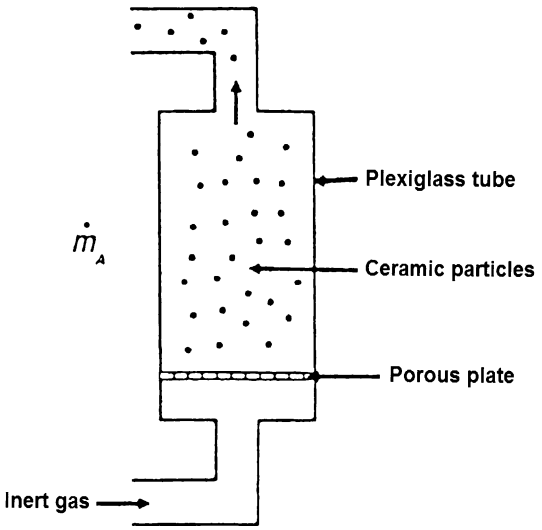

Fig. 20 Schematic of the fluidized bed used in the variable co-deposition technique [121]

A modified spray atomization and deposition set-up is shown in Fig. 21 [160, 161]. The experimental set-up, shown in this figure, incorporates a series of pressure transducers and thermocouples coupled with pneumatic control of the deposition surface. The pressure transducers are used to monitor and control the gas atomization pressure, the chamber pressure, and the instantaneous position on the deposition surface. The thermocouples aid in monitoring (i) the temperature of the melt, (ii) the temperature of the nozzle, and (iii) temperature of the deposition surface, during the experiments.

During spray atomization and deposition, the matrix material is disintegrated into a dispersion of droplets; the average size is denoted by d_{50}, using high-velocity inert gas jets. Concurrently, fine ceramic particulates are co-injected into the atomized spray at a previously determined spatial location (say Z_i) and at an angle. The injection distance is determined based on a numerical analysis of the fraction of solid contained in the atomized matrix as a function of the flight distance. The synthesis attempts to achieve careful interfacial control by injecting the reinforcing particulates at a spatial location (Z_i) where the atomized spray contains a limited amount of volume fraction of the liquid. Thus, (i) the contact time, (ii) thermal exposure of the reinforcing particulates with the partially solidified matrix, and (iii) interfacial reactions are all minimized.

The resultant microstructural characteristics of the spray-deposited material depends largely on the conditions of the droplets prior to their one-to-one impact with the substrate, that is, on the following: (i) the relative proportions of liquid and solid phases present, (ii) temperature, (iii) velocity, and (iv) size of the intrinsic microstructural feature in both the partially solidified and fully solidified droplets [161, 162]. It is important to know the size and distribution of the droplets, since the amount of heat dissipated by the droplets during flight is strongly dependent on their size. Overall, microstructure evolution during spray atomization and deposition can be separated into two distinct yet closely related stages.

(a) The first stage encompasses those phenomena that are normally active in the atomized spray prior to its impact with the substrate.

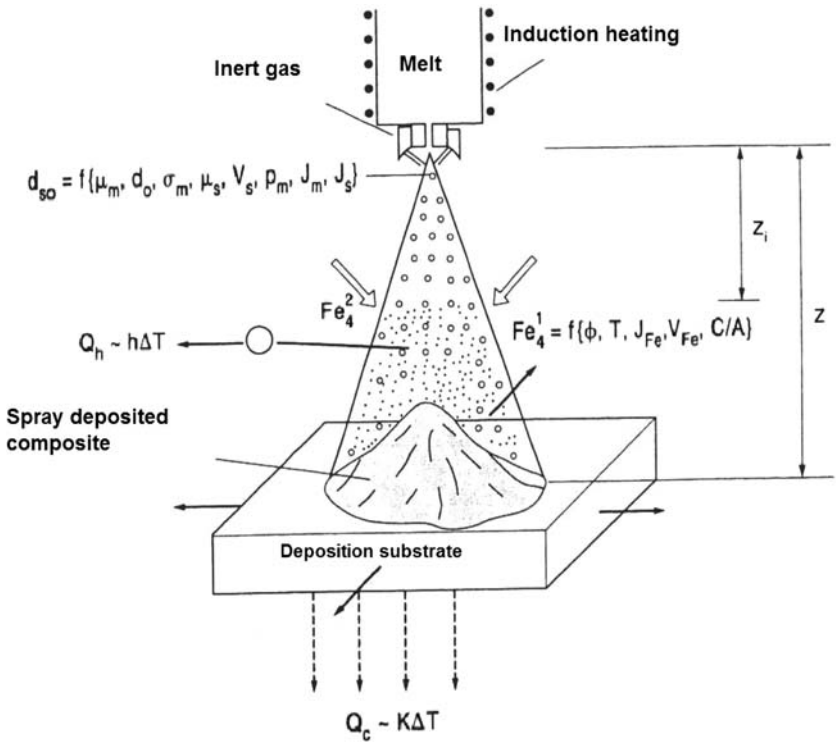

Fig. 21 The experimental arrangement of the spray deposition processing of composite materials [121]

(b) The second stage commences after the droplets have impacted the deposition surface resulting in an alteration of the microstructure upon impact with the substrate.

At the moment of impact of the droplets with the deposition surface, the thermal and solidification conditions governing droplet distribution depend on the following:

(i) the thermodynamic properties of the material used;
(ii) the thermodynamic properties of the gas;
(iii) the processing parameters.

In order to develop a better understanding of the evolution of microstructure subsequent to deposition and impact, it is essential to establish the thermal conditions of the growing deposit.

During the deposition stage, an extensive fragmentation of the dendrite arms formed during solidification occurs because of the repeated impact of the partially solidified droplets, initially with the deposition surface, and subsequently with each other. The presence of dendrite fragments coupled with the development of strong convective currents in the liquid during impact and the formation and presence of a large number of solid nuclei have all been proposed as factors contributing to the development of equiaxed grain morphology during spray atomization and deposition [160–163]. The spheroidal or "equiaxed" grains, referred to as spheroidal in most related studies in order to distinguish it from the equiaxed grain morphology that is generally present during convectional solidification, a feature that is consistently observed regardless of alloy composition. It is accepted that the formation of this microstructure is intimately linked to the solidification conditions that are present during atomization and deposition.

In an exhaustive study on nickel aluminide (Ni_3Al) powders, it was proposed that the formation of equiaxed grains from the dendrites during annealing evolves from two distinct mechanisms [163]:

(a) the coarsening of secondary dendrite arms, and
(b) the growth and coarsening of the primary dendrite arms.

During the early years in an attempt to comprehensively understand, the solidification kinetics during spray atomization and deposition a nickel aluminide (Ni_3Al) was selected as an experimental material because of interest in this class of alloys for elevated temperature applications [164, 165]. In order to characterize the thermal history of the material during processing, the temperature inside the deposit was measured by placing a Type-C (Tungsten–5% Rhenium vs. Tungsten–26% Rhenium, temperature range of 273–2,593 K and a lag time of 0.9 s) thermocouple at a location that was 10 mm from the substrate surface.

Microstructural characterization studies conducted on the spray-deposited material showed that the Ni_3Al deposit

consisted of three distinct regions of different microstructures [166]. In a region located near the substrate, the microstructure consisted of densely packed powders that deformed upon impact with thick-prior droplet boundaries between them, giving the region a highly irregular appearance. Locally, the microstructure inside the deformed powders consisted of a mixture of deformed dendrite arms, fractured dendrite arms, and what appeared to be dendrite arms aligned perpendicularly to the deposition surface. In general, microstructural observations made in this region suggest the droplets to be partially solidified upon impact with the deposition surface. The dendrites that were examined in this region appeared to have experienced either extensive plasticity or fracture. Based on work reported elsewhere suggesting that the deformed or fractured dendrites to have a large orientation misfit with the primary and/or secondary arms [167], the deformed or fractured dendrite arms were considered as independent grains.

A large fraction of the microstructure in the deposited material consisted of fine, homogeneous, and fully spheroidal grains with an average size of 10.7 μm. The microstructure appeared to be reasonably dense with a porosity of 1.3 vol.%. The spheroidal grains present in the region were not fully developed, and their size distribution was heterogeneous.

Kinetics governing microstructural evolution during atomization

The microstructural characteristics of spray atomized and deposited materials are critically dependent upon the solidification history of the droplets during atomization. It is well documented that the solidification behavior of atomized metal droplets is strongly dependent on the following: (i) the distribution of droplet size, and (ii) the flow and thermal interactions with the atomization gas. During atomization, droplets form because of momentum transfer from the gas to the liquid, promoting the formation of ligaments that eventually acquire a spherical morphology because of surface tension forces [167, 168]. The spheroidization of ligaments is particularly rapid in molten metals because of their high surface tension [169]. Therefore, it was assumed that the droplets are spherical. The atomization gas not only provides the energy to disintegrate the liquid metal into micron-sized droplets, but also provides a cooling medium for the droplets. The disintegration and cooling of the droplets are intimately related to the exit gas properties of velocity, density, and temperature. The rapid extraction of thermal energy resulted in the classification of liquid metal atomization as a "rapid solidification" process. One of the key characteristics of rapid solidification is the attainment of relatively high levels of undercooling prior to the onset of nucleation. Although the nucleation may take place heterogeneously or homogeneously, heterogeneous nucleation governs solidification in almost all practical cases [170].

It is important and useful to have knowledge of the undercooling that is required for homogeneous nucleation, as an upper bound of the maximum level of undercooling achieved. If all of the droplets were to nucleate and solidify homogeneously, then the N droplets should exhibit the same level of homogeneous undercooling. However, the presence of nucleation catalysts will promote or favor heterogeneous nucleation in a proportion of the incoming droplets, defined as N_h. Thus, the number of droplets that nucleate homogeneously is reduced to $(N - N_h)$. If the undercooling required for heterogeneous nucleation is assumed negligibly small when compared to that which is required for homogeneous nucleation, then heterogeneous nucleation is initiated and occurs to completion.

The droplets arriving on the deposition surface are either in the fully solid, liquid, or partially solid condition. Further, the fine dendritic microstructures that are present in the powders provide experimental support to the relatively fast rates of heat extraction that were computed based on thermal considerations. However, it was evident that there existed significant microstructural variations within a single droplet, both in scale and morphology, owing to the complex thermal history experienced by the droplet, that is, a combination of undercooling, nucleation, recalescence, and equilibrium solidification. This highly heterogeneous mixture of microstructures arrives on the deposition surface, eventually collecting as a highly dense preform, whose microstructure critically depends on the following: (a) solidification characteristics of the impinging droplets, (b) the interactions of the droplets with the deposition surface, and (c) mutually interactive with each other. Overall, a large proportion of the microstructure present in the spray-deposited nickel aluminide (Ni_3Al) exhibited spheroidal grain morphology. Other investigators have reported the presence of spheroidal grain morphology for spray atomized and deposited aluminum and magnesium alloys [27]. Mild steel and tool steels [171], nickel-based alloys [172], copper alloys [169], and even MMCs [137, 173–176].

The overall cooling rate experienced by the spray is greater than 10^4 K/s, whereas the cooling rate experienced by the deposited billet is several orders of magnitude less when compared to the spray. The cooling rate is essentially controlled by the conjoint and mutually interactive interactions with each other of the following:

(a) the deposit-substrate heat transfer coefficient;
(b) thermal properties of the material.

The low cooling rates will effectively expose the spray-deposited material to an elevated temperature anneal for a finite amount of time. Elevated temperature annealing of the spray-deposited material is conducive for the occurrence of grain growth and eventual coalescence, resulting in the formation of a spheroidal grain microstructure during subsequent annealing by two distinct yet interactive mechanisms: (i) a homogenization of the dendrites that did not deform extensively during deposition, and (ii) the growth and eventual coalescence of the deformed and fractured dendrite arms. This is shown in Fig. 22.

Based on elevated temperature annealing studies the grain growth kinetics of spray-deposited nickel aluminide during annealing is obtained from the relationship:

$$D^2 - D_o^2 = 1.44 \times 10^{11} \exp(-33{,}800/T)(t), \quad (8)$$

where D is the average diameter of the dendrite fragments or spheroidal grains, D_o the initial average diameter of the dendrite fragments; T the annealing temperature, and t the annealing time. With this relationship, the grain size at a certain annealing temperature and time can be predicted, that is, if the annealing temperature and grain size are fixed, the annealing time can be predicted. An increase in annealing temperature (T) corresponds to an increase in time needed for the grains in the deposited material to grow to a particular size.

The formation of a non-dendritic, spheroidal morphology during spray deposition has been attributed to factors such as an extensive fragmentation of the dendrite arms in the partially solidified droplets during its impact with the substrate [149, 163, 177–179], a comprehensive investigation of this phenomenon was lacking. In an attempt to better understand and rationalize this phenomenon Liang and coworkers [180, 181] subjected a nickel aluminide (Ni_3Al) intermetallic to atomization using nitrogen gas at a dynamic pressure of 2.41 MPa and a melt superheat temperature of 1,823 K. The mass flow rates of the atomizing gas and liquid melt were adjusted to be 0.022 and 0.078 kg/s. The copper deposition surface was water cooled and positioned at a distance of 25.4 cm from the atomization nozzle. The overspray powders were collected in a cyclone separator for purpose of analysis. The atomized nickel aluminide (Ni_3Al) powders exhibited a typical rapid solidification microstructure consisting of fine dendrites of the single long-range gamma-prime (γ') ordered phase [182]. The micron-sized dendrites exhibited well-defined primary and secondary arms. The observed fine scale of the microstructure was attributed to the fast solidification front velocity resulting from the highly non-equilibrium conditions that are present during atomization [61]. The extent of microstructural refinement, as measured by spacing of the secondary dendrite arms (SDAS), was found to be inversely related to the diameter of the powder particles. The variation of experimentally measured SDAS with diameter of the powder particle is shown in Fig. 23. The thermal profile of three locations inside the spray-deposited material (Fig. 24) was measured and recorded and the results are shown in Fig. 25, together with the liquidus and solidus temperatures of the nickel aluminide (Ni_3Al) used in this study. The results reveal the temperature at all three locations of the spray-deposited material to remain below the solidus temperature. From this data, it was inferred that the

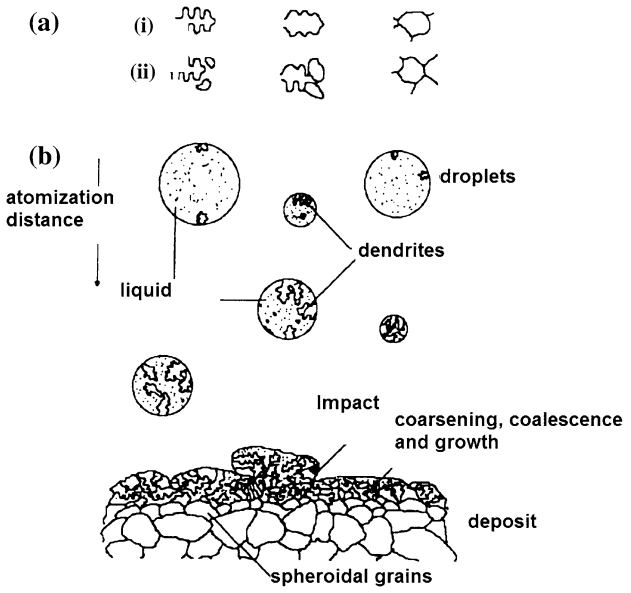

Fig. 22 **a** Mechanism leading to the formation of spheroidal grains during annealing: (i) homogenization of the dendrites that did not deform extensively during deposition, (ii) the growth and coalescence of the deformed and fractured dendrite arms. **b** The formation of spheroidal grains during spray atomization and deposition [177]

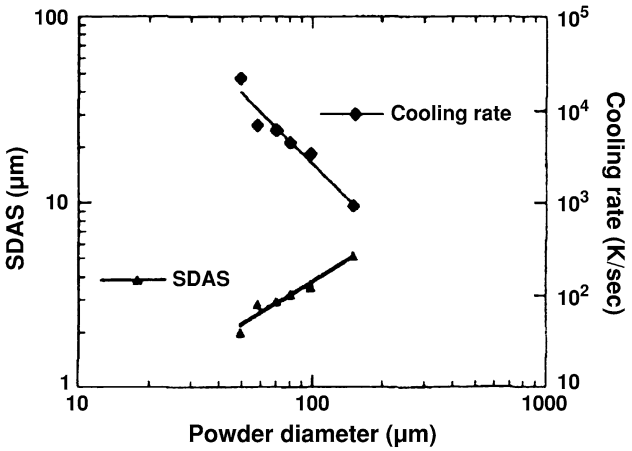

Fig. 23 The effect of powder diameter on the measured secondary dendrite arm spacing (SDAS) and estimated cooling rate of atomized nickel aluminide (Ni_3Al) powders [177]

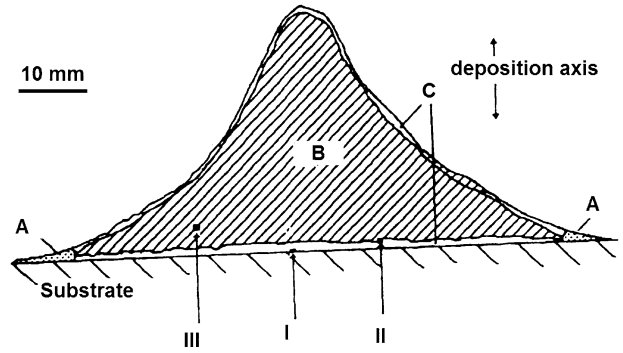

Fig. 24 Cross-section big the spray-deposited billet and the three regions A, B, C, which reveal different microstructural morphology. I, II, and III correspond to positions of the three thermo-couples [177]

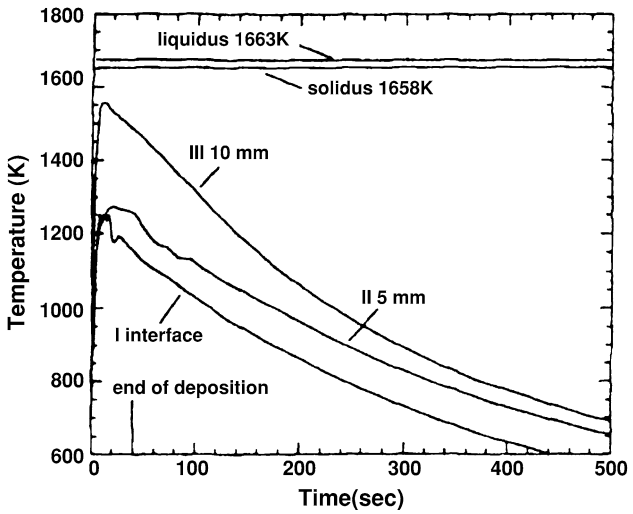

Fig. 25 Measured temperature profiles at three positions inside the deposit billet during spray atomization and deposition of nickel aluminide [177]

average cooling rate that was associated with the high temperature region ($T > 0.5T_m$) was approximately 2.6 K/s. The low cooling rate of the deposit does cause shrinkage to occur at the "local level" in the deposit. While spray processing does have numerous advantages to offer, it must be noted that the process does have a handful of disadvantages. Importantly the process yield causes a loss of about 38 pct. coupled with the difficulty to easily attain near-net shape.

It is to be noted that despite large differences in composition, the spheroidal grain morphology associated with these different materials is very similar, with some differences reported in the amount and distribution of porosity, with grain size variations typically in the range of 10–40 μm. To elucidate the formation of the non-dendritic spheroidal shape grains during spray atomization and deposition, and considering all of the similarities involved, we provide an overview of the formation of equiaxed grains during conventional solidification.

In conventional castings, an equiaxed grain microstructure is generally observed in the center section for almost all types of metallic materials [58, 183, 184]. Columnar dendrite grains that originate at the mold/metal interface surround the equiaxed grain microstructure that is normally present in the central section of castings. Qualitatively, the equiaxed grains are thought to evolve from the re-melting and separation of otherwise columnar dendrites that are subsequently carried into the undercooled melt by convection, where they tend to nucleate new grains. The radial loss of thermal energy (latent heat) from the dendrite fragments to the undercooled melt enhances the formation of equiaxed morphology. Accordingly, the transition from columnar to equiaxed growth was found to be intimately linked to the extent of convection in the liquid. The size of equiaxed grain that is generally associated with this mechanism is relatively coarse (e.g., greater than 100 μm). The formation of the equiaxed grains typically requires a high solid–liquid interface migration velocity, convective fluid flow, and a negative temperature gradient [183, 184].

It is evident that the mechanisms governing the formation of spheroidal grains during spray deposition and specifically spray atomization and deposition will differ from those qualitatively described for equiaxed grains in conventional casting processes. It has been suggested that the spheroidal grain structure typically observed in spray atomized and deposited materials develops from a molten layer that forms during spray deposition [163]. According to the proposed mechanism, the rate of heat extraction at the substrate is lower than the heat input at the upper surface leading to the formation of a molten layer on top of the deposit. Hence, the droplets arriving on this layer may: (a) deform and re-melt, or bounce off, if they are in the solid state, (b) coalesce if completely molten, or (c) fracture if semi-solid thus providing dendrite arms that eventually act as solidification nuclei [163]. In related work by the same researchers [171], it was suggested that the formation of spheroidal grain morphology during spray deposition is enhanced because of three simultaneous processes (a) dendrite arm fragmentation, (b) nucleation/grain multiplication, and (c) constrained growth [175]. Alternatively, it has been proposed that a semi-solid layer develops on top of the deposit because of the repeated impact of a large proportion of partially solidified droplets [175, 179, 185, 186].

Low-pressure plasma deposition

Synergizing the two independent operations of powder synthesis and their consolidation, involved in RSP, into a single step or operation led to the emergence of the

technique of plasma processing. This attractive technology facilitated an achievement of metallurgical and chemical homogeneity and was used for the direct fabrication of a variety of simple preform shapes, such as, (a) tubes, (b) discs, and (c) ingots. Around the same time, a new process was developed by the General Electric Company for net shape processing by plasma spraying in a reduced pressure environment. This technique was called low-pressure plasma deposition (LPPD). Unlike the technique of spray deposition, the unique feature of the LPPD process is that it makes use of pre-alloyed powders as the feedstock coupled with an intrinsic difference in the manner in which the sprayed deposit is built-up into a monolithic shape. The emergence of the LPPD technology led to an availability of quality coatings of high performance materials. The coatings found application in industrial gas turbines and jet engines. Furthermore, an ability to control the deposition of the material at elevated temperatures coupled with sound metallurgical quality facilitated in an increased use of the LPPD technology to build thick (>5 cm) deposits without sacrificing quality.

The low-pressure plasma spray deposition technique combines particle melting, quenching, and consolidation in a single operation. The process involves an injection of a variety of powder particles ranging from metallic to ceramic, and including mixtures, into a plasma jet stream created by heating an inert gas in an electric arc confined within a water-cooled nozzle. The particles injected into the plasma jet, at temperatures of 10,000 K and higher, undergo rapid melting and are accelerated toward the work piece surface. Rapid quenching of the molten particles occurs when the droplets impact with the substrate. The cooling rates are very high, of the order of 10^5–10^6 K/s, and the resulting microstructure is fine-grained and homogeneous. Compared to other RSP approaches, plasma spraying offers the advantages of: (i) large throughput (kg/h), (ii) high density, and (iii) an ability to deposit objects of complex shape and to even produce near-net shape bulk forms.

The technique of conventional plasma spraying (CPS) is normally carried out at atmospheric pressure. The resultant deposit contains oxidation products together with some porosity due to incomplete melting, wetting, or fusing together of the deposited particles. The problem of oxidation is overcome or minimized by either shielding the plasma-arc in an inert gas atmosphere, or by enclosing the entire plasma spraying unit in an evacuated chamber, which is maintained at about 30–60 torr inert gas pressure by high speed pumping. Under the operating conditions of LPPD, the gas velocities are high (typically in the Mach 2–3 range) due to the higher permissible pressure ratios. When the inert gas environment is entirely vacuum, the technique is referred to as vacuum plasma spraying (VPS). Other noteworthy advantages of low-pressure inert gas deposition also known as VPS, when compared with CPS, include the following [138–140, 187]:

(a) higher particle velocities, which give rise to dense deposits (often> 98% of theoretical density);
(b) broad spray patterns, which produce large areas of relatively uniform deposition characteristics;
(c) automatic regulation of the technique to produce controlled deposits having complex geometries at reasonably high-deposition rates (up to 50-kg/h).

The four basic components of a typical plasma gun, namely: (a) cathode (b) arc chamber (c) throat, and (d) exit nozzle, are shown in Fig. 26 [187, 188]. The cathode and anode are located concentrically and are water cooled for preventing melting by the high gas temperatures. An arc gas (argon or a mixture of argon and helium) is fed from behind the cathode. The arc gas is fed tangentially, thereby creating a vortex that acts to stabilize the electric arc. The powder injection ports are located either within the nozzle (anode) or downstream of the nozzle, depending primarily on the characteristic of the plasma gun, and the type of powder being sprayed.

Protection against environmental interactions after particle melting has occurred is achieved by injecting a shroud of inert gas around the periphery of the jet and/or around the substrate. The bare minimum amount of the inert gas environment ensures that the particles and droplets are protected from oxidation. By minimizing environmental interactions, high-quality metallurgically sound deposits, which are well bonded to the substrate, are achieved by the low-pressure inert gas spraying technique.

The fine metal particles are injected into the plasma flame, where they are melted and accelerated to high

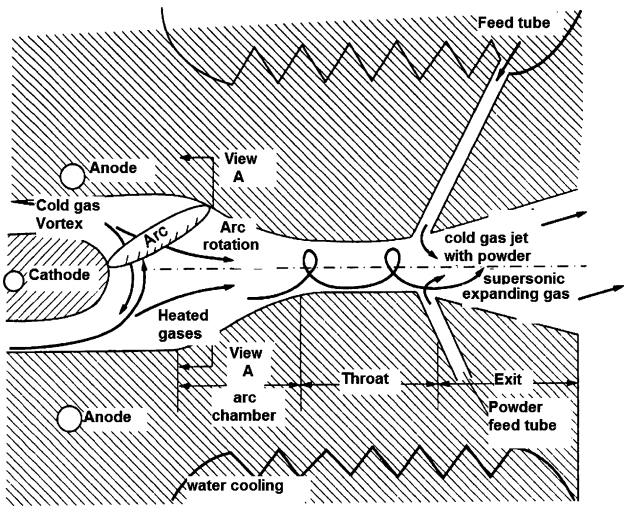

Fig. 26 Cross-sectional schematic of the plasma gun showing the supersonic expanding gas jet [187, 188]

velocities (200–300 m/s) towards the substrate. The particles impact the substrate and rapidly solidify. A rapid solidification rate (RSR) deposit is built-up by the successive impingement of molten particles. During the course of deposition processing, the substrate-deposit system is exposed to temperatures of 800–900 °C, due to an interaction with the hot plasma flame and the heat of solidification. The resultant annealing, arising from the high temperature exposure, was found to be beneficial, since it provided stress relief to the deposit, improved interparticle bonding, and promoted recrystallization to occur without appreciable grain growth, thereby retaining most of the characteristics of RSR processing [189].

The resultant deposits, of the low-pressure plasma spraying process, typically have fine microstructures and contain varying amounts of retained porosity and inclusions, depending on deposition parameters, such as (i) power level, (ii) arc gas composition, (iii) jet transport properties, and (iv) level of reduced pressure. The protected atmosphere minimizes the number of oxide-containing inclusions and the number density of pores. The resultant deposit contains fewer inclusions and the density achieved under conditions of low-pressure plasma spraying is about 98% of the theoretical density.

The first use of the LPPD or VPS technique for superalloys resulted in a noticeable improvement in strength. This was attributed to the synergistic and competing influences of microstructural (grain size) refinement, microstructural homogeneity coupled with extended solubility of the solid solution strengtheners.

Modified gas welding technique

In this technique, the gas metal arc (GMA) welding torch is modified, wherein, aluminum or aluminum alloy wire feedstock is melted and combined with silicon carbide particulates (SiCp) or silicon carbide whiskers (SiCw) entrained in an inert gas. Upon striking a substrate or mold, the mixture of aluminum alloy and silicon carbide (SiC) particulates solidifies into a composite structure [141]. A schematic of the deposition process is shown in Fig. 27.

An arc when struck between the end of the aluminum wire and a water-cooled copper cathode produces a stream of droplets about 1 mm in diameter. At about 230 Amps, the melting rates are about 2 kg/h. The thermal history of these droplets is controlled to some extent by the electrical parameters of the melting process, the shielding gas used, and the distance from the orifice to the mold or substrate [141]. Thermal control of solidification is affected by thermal properties of the mold or substrate. At any instant of time, very little liquid is present, adequate to bond successive droplets and the reinforcing phase. In this technique, the reinforcement material is not substantially

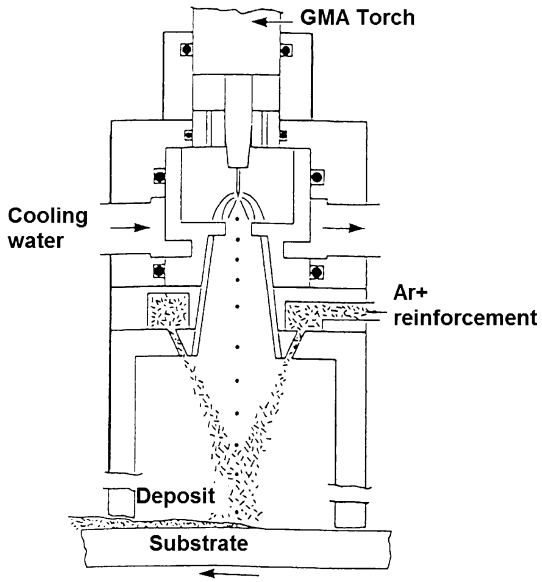

Fig. 27 A schematic of the modified gas metal arc welding deposition process [141]

affected by fluid flow and macro-segregation during solidification. Using appropriate molds and substrates, complex parts and near-net shapes of a uniform composite structure can be produced. The process has been developed into a welding technique for metal-based composites that would provide the weld metal of approximately the same composition as the base material, thereby reducing the need for mechanical fasteners and adhesives in the fabrication of large structures.

The advantages of the gas welding technique are manifold and include the following [141]:

(i) an ability to melt, by the arc, any metal, including the very high temperature alloys;
(ii) an ability to entrain any reinforcement in the shielding gas, thus providing a wide variety of reinforced metallic matrices or composite materials;
(iii) melting is more convenient than conventional melting methods, since it can be turned on and off with relative ease;
(iv) an ability to produce large droplets, thereby, minimizing the explosion hazards associated with finely divided aluminum powder;
(v) most importantly, the modified GMA torch is compact, inexpensive and controllable.

Overall, the modified gas welding technique is stable and can be operated for several minutes, with controllable termination as the end of the substrate is approached. The potential problems arising from the operation of this process include clogging of the orifice, arc instabilities, and arc extinction due to gas flow imbalances. For the process to be successful, proper shielding of the droplet stream and

solidifying metal are both important and essential in order to produce a good surface finish while concurrently keeping internal porosity at a low level. With a high-quality matrix coupled with the intrinsic capability of adding variable amounts and kinds of reinforcing phases, this processing technique facilitates appropriate microstructural control of MMCs.

High-velocity oxyfuel spraying

High-velocity oxyfuel thermal spraying is the most significant development in the thermal-spray industry since the development of plasma spraying. The rapid growth of this technology was attributed, to a large degree, to the extensive development of materials and equipment following the introduction of the Jet Kote HVOF spray process in 1982 [142, 143]. The early years saw the technique being used exclusively for aircraft/aerospace applications and even part reconditioning. However, with advances in time, the applications of HVOF have expanded from the initial use of tungsten carbide coatings to include hundreds of different coatings that provide for wear, erosion and/or corrosion resistance, restoration, and even clearance control of components [142]. A wide variety of coating materials have been sprayed using the high-velocity oxy-fuel thermal-spray technique. However, the process has found concentrated use for the application of carbides (tungsten and chromium carbides).

The HVOF thermal spraying process uses an internal combustion (rocket) jet to generate hypersonic gas velocities of 1,830 m/s, more than five times the speed of sound. Some of the combustion fuels include (a) propylene, (b) acetylene, (c) propane, and (d) hydrogen gases for the spraying of carbide and even non-carbide coating materials. When burned either in an atmosphere or in combination with pure oxygen, these fuels produce gas temperatures greater than 2,760 °C [5,000 F]. The high-velocity oxy-fuel gun is shown in Fig. 28.

The flow of powder is electrically controlled and the feed rates are monitored automatically. The powders deposited using the HVOF thermal-spray process include pure metals, their alloy counterparts, carbides, certain ceramics, and even plastics. The early use of the HVOF thermal-spray technology was for carbide coatings on aircraft gas turbine engine components, which experienced wear from abrasion, adhesion, erosion, fretting and corrosion. The key parameters influencing the wear resistance of carbide coatings are flame temperature and particle velocity. An additional advantage of this spraying technique is that the tungsten carbide coatings produced are better than those obtained using plasma synthesis in terms of higher hardness, higher coating bond strength, lower oxide content and porosity, and improved wear resistance in combination with low residual stress in the coating. The microstructure resulting from HVOF spraying are equal to, or better than, those of the highest quality plasma sprayed coatings, The HVOF coatings show no cracking, spalling or delamination after heating to temperature as high as 1,095 °C [2000 F] in air and quenching in liquid Freon.

Notable applications of the technology of RSP

During the last two decades, numerous studies have been systematically conducted by few researchers working exclusively in this area with the objective of understanding the innate capability to spray process numerous metals, alloys and their composite counterparts. The ultimate objective of these studies was to rationalize processing influences on microstructural development and the

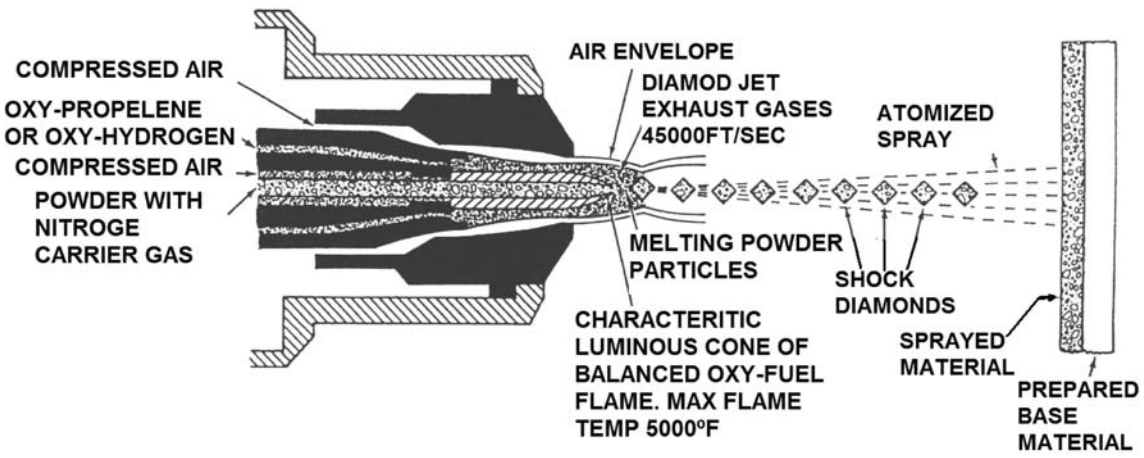

Fig. 28 Schematic showing cross-section of the high-velocity oxy-fuel gun [142]

resultant influence of microstructure on mechanical properties. Five selected studies are chosen and independently presented and discussed.

Understanding solidification characteristics of aluminum–titanium powders

This study was undertaken with the objective of providing an insight into solidification microstructures and segregation patterns that are present in micron-sized aluminum–titanium powders, with an emphasis on understanding the synergism between microstructure and processing [190]. The aluminum–titanium alloy was obtained by mixing an Al–6.0 wt% titanium master alloy with commercial purity aluminum [99.99% pure]. The two master alloys were mixed in order to obtain a target alloy composition of Al–5.1 wt% titanium. In an attempt to ensure dissolution of the primary Al_3Ti intermetallic phase and to promote sufficient mixing during melting, the alloy was slowly heated, in a nitrogen atmosphere, in a zirconia crucible to the desired superheat temperature. The melt was maintained at the superheat temperature for approximately 10–20 min prior to atomization. The liquid melt was then disintegrated into a fine dispersion of micron-sized droplets using nitrogen gas at a pre-selected pressure. Following atomization, the rapidly quenched powders were separated from the atomization gas using a cyclone separator. To avoid extensive oxidation of the aluminum–titanium alloy during processing, the experiments were conducted inside an environmental chamber [190]. The environmental chamber was evacuated down to a pressure of 15 μm of Hg and back filled with inert gas (nitrogen) prior to melting and atomization. An exhaustive examination of the solidification morphology revealed that there were three types of microstructures to be present in the atomized powders. In powders less than 10 μm in diameter, the microstructure was often featureless, and no dendrites or cells were evident (Fig. 29a). In powders with a diameter larger than 10 μm, but smaller than 100 μm, the microstructure exhibited a cellular morphology (Fig. 29b). In powders larger than 100 μm, the microstructure was typically dendritic (Fig. 29c). In most of the powders, the solidification

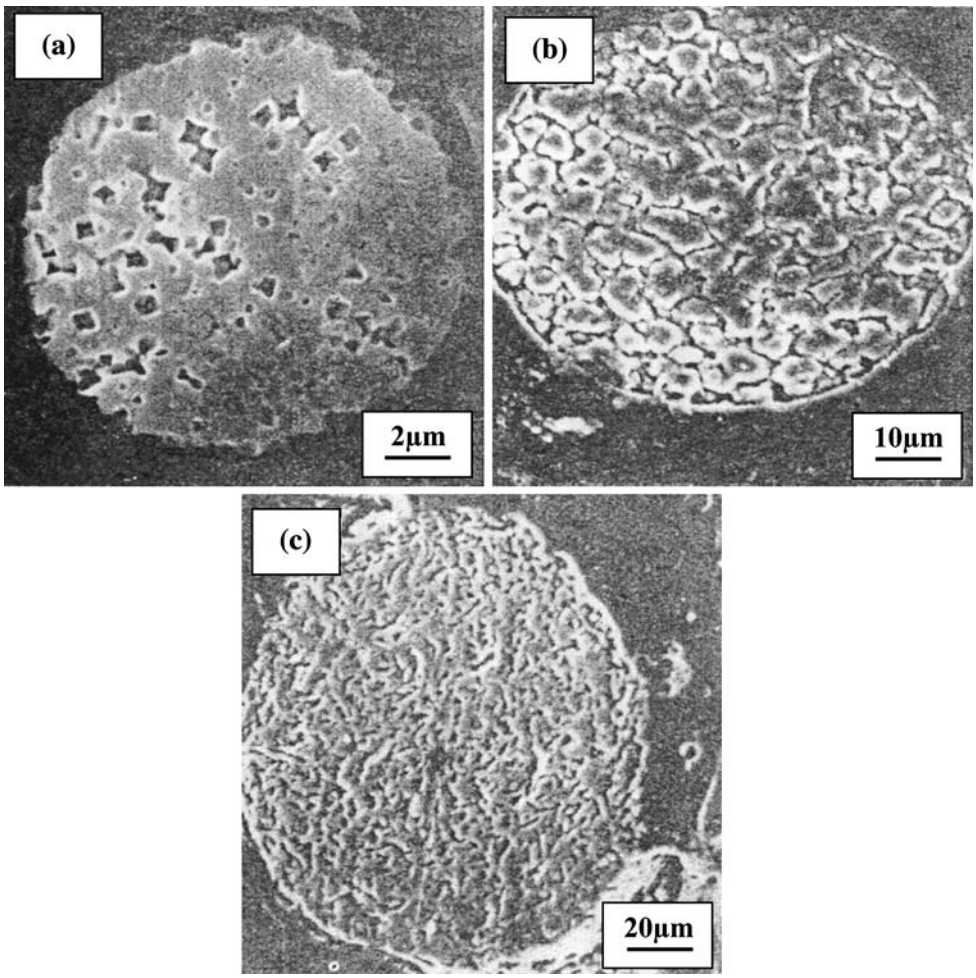

Fig. 29 Scanning electron micrographs showing the following **a** featureless microstructure for powders less than 10 μm, **b** cellular solidification morphology for powders in the size range 10–100 μm, and **c** dendritic microstructure for powders greater than 100 μm in diameter [190]

microstructure was clearly indicative of multiple nucleation events. The segregation patterns obtained for the powders of diameter less than 10 μm indicated that solidification during atomization initiated at the surface.

Evaluating precipitation kinetics and solid solubility in magnesium alloys processed by spray atomization and deposition

Magnesium is one of the lightest structural materials known to humankind. When compared one-to-one with currently available structural materials, magnesium is an attractive alternative because of its unique combination of low density and excellent machinability [191–193]. Although the magnesium alloys do not compare favorably with aluminum alloys in terns of mechanical behavior, their low density (35% lower than that of aluminum) makes them highly competitive in terms of strength–density values. However, its poor oxidation and corrosion resistance, low thermal stability, poor forming characteristics and relatively low strength levels, have hampered the widespread use of magnesium alloys. The advent of RST enabled in the development of magnesium alloys that offered attractive combinations of structure and properties. The rapidly solidified magnesium alloy particulates must be consolidated to full density before they can be useful as structural material. This involves the combination of canning, cold pressing, degassing, and final forming. However, a combination of highly reactive material such as magnesium and aluminum coupled with the high surface area associated with RST processes makes it impossible to avoid the formation of oxide phases during spraying and consolidation. This study was undertaken to provide an insight into the processing of magnesium alloys by spray atomization and deposition, with particular emphasis on microstructure development and the precipitated phases [194]. The two magnesium alloys chosen for this study were Mg–Zn–Zr and Mg–Al–Zr [194]. The purpose of choosing the zirconium containing alloys was that zirconium improves grain size control resulting in increased strength levels due to interference hardening mechanisms [195]. The microstructure of the spray atomized and deposited material from a series of experiments conducted consisted of equiaxed cells, 30–80 μm in diameter with the occurrence of second-phase precipitation in both materials. The maximum cell size observed in the Mg–Zn alloy was approximately 80 μm. Further, numerous prior droplet boundaries were readily discernible throughout the microstructure (Fig. 30). The near equiaxed cell morphology became apparent only after extensive etching. The microstructure of the Mg–Al alloy was characterized by an average cell size of 40 μm and by the absence of prior droplet boundaries. Essentially the cell morphology of the magnesium alloys consisted of pre-solidified droplets and splats. The cell boundaries were evident after extensive etching. The cell morphology of the

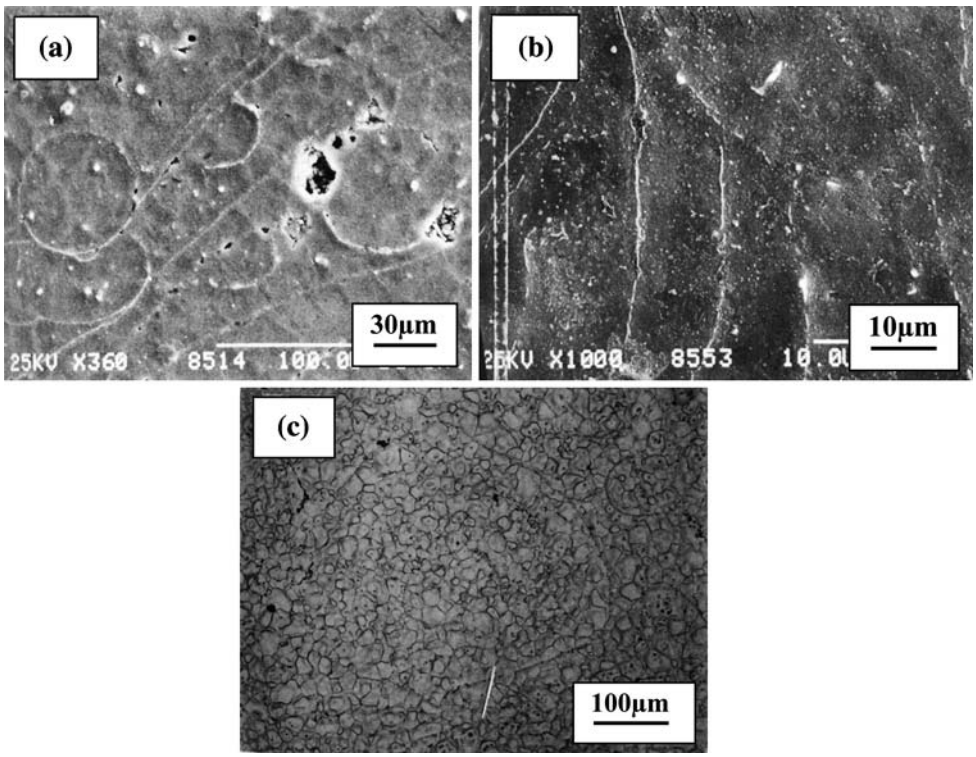

Fig. 30 Scanning electron micrographs showing the as-spray-deposited microstructure of the Mg–Zn alloy showing: **a** longitudinal section, **b** transverse section, **c** optical micrograph showing equiaxed cell morphology. These micrographs were taken from the central region of the spray-deposited material [194]

Mg–Al alloy was mostly equiaxed. The presence of equiaxed cell morphology is in agreement with the findings put forth by other investigators [122, 196–202]. However, the noticeable absence of equiaxed cell morphology throughout some regions of the Mg–Zn alloy was attributed to a large proportion of the pre-solidified droplets arriving at the substrate. The relatively high volume fraction of solid present upon impact with the substrate prevented extensive fragmentation of the droplet-dendrite. Consequently, a large proportion of the droplets retained their spherical morphology after impact with the substrate.

The precipitation of secondary phases, the presence of the Mg_7Zn_3 phase in the Mg–Zn alloy is not unexpected since the Mg_7Zn_3 phase is in equilibrium with magnesium at the eutectic temperature. The absence of detectable amounts of the MgZn phase was attributed to the lack of time for the occurrence of solid-state transformation ($Mg_7Zn_3 = 3MgZn + 4Mg$) to take place. The decrease in grain size coupled with a reduction in the size and amount of secondary phases present in the spray-deposited material, relative to that present in the cast and hot rolled microstructure, are a direct result of the relatively high rates of heat extraction present during spray atomization and deposition processing. Initially, when the material begins to solidify, either in the powder form or as part of the growing preform, the primary magnesium-rich solid solution should form. Solidification is slow enough to allow for segregation of aluminum into the liquid. As the solidification front advances, the magnesium-rich solid solution that is being formed contains increasing amounts of aluminum ("coring"). Eventually, the aluminum concentration in the melt surrounding the solid cellular grains is high enough that eutectic solidification takes place. The eutectic makes its presence in the microstructure in the form of a "divorced" eutectic.

Understanding high-pressure spray atomization of palladium–rhodium alloys

There exists a beneficial synergistic and intrinsic quality between PM and rapid solidification, since the powders made by spray atomization techniques are subject to the cooling rates that fall within the rapid solidification regime [203]. Palladium and its alloys are of engineering interest because of their unique hydrogen absorption/desorption characteristics [204]. Technological applications resulting from these unique characteristics include the use of palladium and its alloy counterparts as catalysts in the processing by organic synthesis, hydrogenation, and dehydrogenation as hydrogen purification diaphragms and as a hydrogen storage material [204, 205]. In the case of rhodium, its addition of up to 20 wt% to palladium has a considerable influence on properties through direct improvement, but also has the unique characteristic in that it does not lead to a decrease in the limiting amount of hydrogen uptake at accessible hydrogen pressures, as the other substitution elements normally do. The segregation behavior of palladium–rhodium (Pd–Rh) alloys plays an important role in hydrogen absorption [206]. Consequently, high-pressure gas atomization involving rapid solidification is typically used to provide solidification condition to minimize the extent of segregation. A Pd–10 Rh alloy was chosen [206, 207]. To prevent freeze-up of the nozzle, the melt was superheated to 100–150 °C prior to the initiation of atomization. The Pd–10 Rh alloy was super-heated to 1,710 °C, and the temperature of the melt was monitored using a thermocouple protected with an alumina sleeve. Once the desired temperature was achieved, the molten metal was tapped through the bottom of the crucible. Successful atomization was performed using an atomization pressure of 1,000 psi (6.89×10^6 Pa). The chamber pressure during atomization was held at 2 psi (1.38×10^4 Pa). The resultant droplets following spray deposition are spherical (Fig. 31). The atomized Pd–Rh powders exhibited a typical rapid solidification microstructure consisting of fine dendrite morphology. The micron-sized dendrites exhibited well-defined primary and secondary arms, and the scale of these dendrites varied as a function of powder size. The fine scale of the microstructure suggests the existence of fast solidification front velocities resulting from highly non-equilibrium conditions present during atomization [208]. A measurement of the SDAS revealed it a function of the corresponding powder diameter (Fig. 32). Further, it was found that the concentration of Pd and Rh is relatively homogeneous in the entire powder.

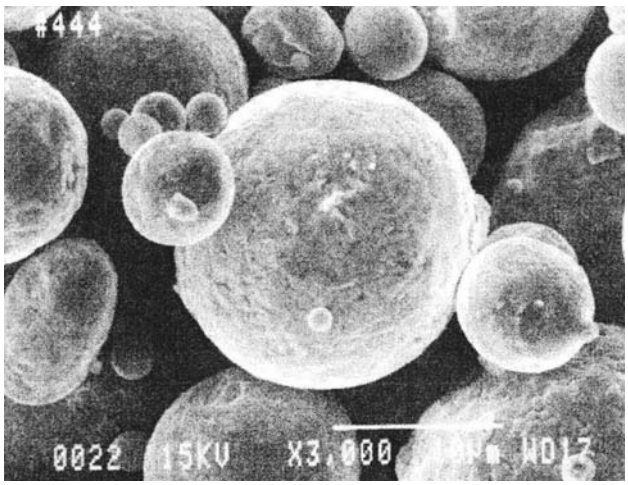

Fig. 31 A scanning electron micrograph of the Pd–Rh atomized powders [208]

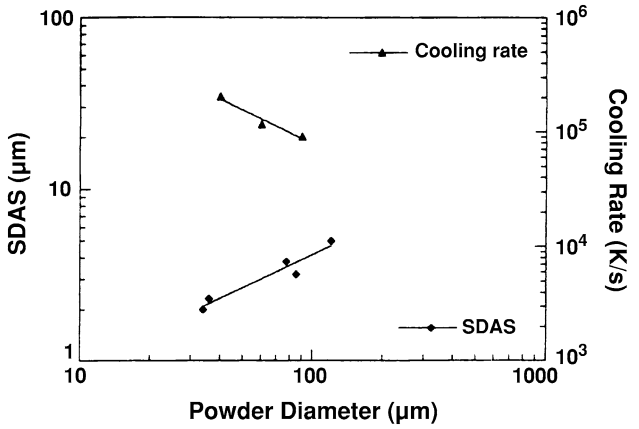

Fig. 32 Calculated cooling rate and measured secondary dendrite arm spacing (SDAS) in the gas atomized Pd–Rh powders during solidification [208]

Evaluating solute segregation behavior in spray-atomized Pd–Rh–V (Co) powders

This study attempted to investigate the solute segregation behavior in spray-atomized Pd–Rh–V powders. This is because a thorough understanding of the solute segregation that occurs during rapid solidification, as in spray atomization technique, is an important aspect of solidification science and technology. The solute segregation in the atomized powder was experimentally investigated using electron probe X-ray microanalysis (EPMA) with wavelength-dispersive spectroscopy (WDS) by determining the chemical composition as a function of position across the powder particle. The solute segregation that occurs during solidification was observed to originate from the initial compositional difference between the solidifying liquid and the solid. When a liquid with solute concentration (C_L) is solidified under near-equilibrium conditions, the solute composition in the solid will be $C_S = k_e C_L$, where k_e is a constant termed as the partition coefficient or more appropriately as the equilibrium partition coefficient [88]. Because of the difference between C_S and C_L, the liquid will become more and more enriched (when $k_e < 1$) or depleted (when $k_e > 1$) in solute as the solidification continues. Consequently, the solute composition in the solid that is formed earlier will be different from that formed latter, resulting in solute segregation in the solidified material [88]. The solute segregation can be minimized or suppressed through either an external method, such as agitation of the melt during solidification, or an internal method, such as rapid solidification [88].

The initial step in the solidification of a liquid is the formation of at least one solid nucleus, i.e., nucleation [88, 209]. The nucleation can be categorized as being either homogeneous or heterogeneous, depending on how the nucleus is formed. When the nucleus is formed by local atomic fluctuations in the melt is termed as homogeneous. However, when it forms by an attachment of the solid atoms onto the surface of a pre-existing, heterogeneous solid material, the nucleation is termed as heterogeneous. The solid material that is conducive to facilitating heterogeneous nucleation is termed a heterogeneous nucleants. The common heterogeneous nucleants being the walls of the container containing the melt and the presence of inclusions or impurities in the melt. In either of the two types of nucleation processes, a certain level of undercooling (difference between the liquidus temperature (T_L) and the nucleation temperature (T_N) will be present. The undercooling encountered in these two types of nucleations is correspondingly termed as homogeneous undercooling and heterogeneous undercooling. For the same material, the heterogeneous undercooling is smaller, at times noticeably smaller, than a homogeneous undercooling [88, 209].

In this specific study, two palladium-based ternary alloys, i.e., Pd–4.9Rh–0.72V and Pf–5Rh–1Co, were spray atomized into micron-sized powders using a high-energy gas atomization technique. The occurrence of solute segregation in the spray-atomized powders was investigated. It was found that with a decrease in powder particle size, the solute segregation level decreases, either in terms of standard deviation of solute content from an average value, or in terms of the percentage of segregation-free regions in the powder, or in terms of the maximum (Rh)/minimum (Co,V) solute content in the powder. Theoretical analysis was carried out to evaluate the percentage of segregation-free regions, as well as the maximum/minimum solute content in each powder. The theoretical analyses revealed that among the different mechanisms governing solute segregation behavior, the undercooling levels experienced by the droplets, both prior to and after nucleation, played an important role in decreasing the solute segregation level with a decrease in size of the powder.

The role of nucleation and growth phenomena on microstructural evolution during droplet-based deposition

In this study, the heat transfer behavior of individual droplets is coupled with the nucleation and growth kinetics during flight and deposition [210]. The nucleation and growth of the individual droplets during flight were evaluated and stored. During deposition, the continuous growth of the existent nuclei was constantly tracked according to the relevant growth kinetics. Concurrently, the possibility of nucleation within the remaining liquid was analyzed in terms of the classical nucleation theory. At the completion of solidification, (i) the size of the nuclei at the time of

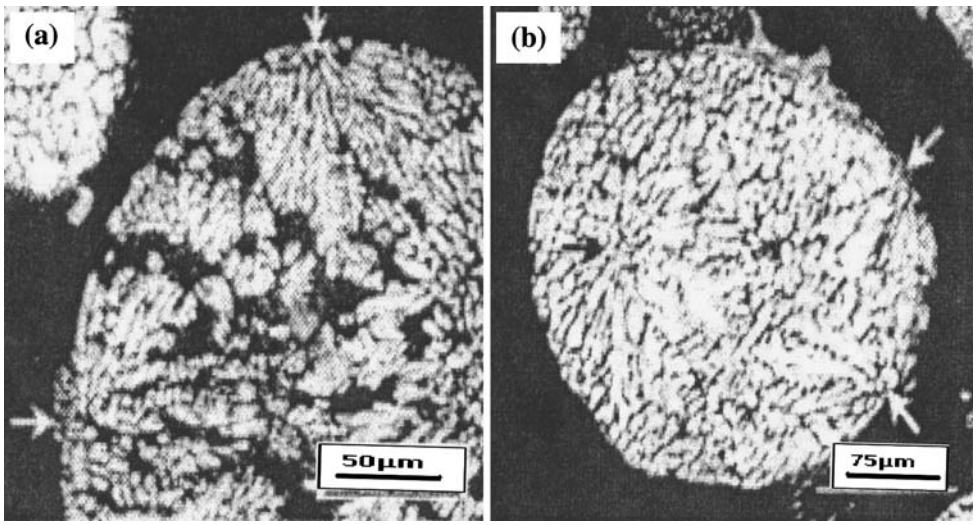

Fig. 33 Microstructure of atomized powders of aluminum alloy 7150 [210]

origination of flight, and (ii) the size and distribution of the nuclei generated during deposition, were obtained. In doing the needful calculations, no artificial undercooling and recalescence was assumed. The degree of undercooling the recalescence process were determined based on the nucleation and growth kinetics, as well as a competition between the release of latent heat during solidification and the dissipation of thermal energy in a droplet.

In this connection, the microstructure of atomized aluminum alloy 7150 powders was examined (Fig. 33). A copper plate intercepted the powder particles of the aluminum alloy during spray forming. It was observed that two nucleation events originate at the surface of the particle and subsequently the primary dendrite arms develop in a fan shaped manner until they impinge on other dendrite arms. A cross-section of the powder particle reveals three nucleation events, two on the surface of the particle and one in the interior. The nucleus within the interior grows radially into the surrounding liquid. Observations of a large number of atomized powders revealed the occurrence of heterogeneous nucleation on the surfaces of the powders to be the dominant mechanism although heterogeneous nucleation in the interior of the powders was also observed to occur. The catalytic centers for heterogeneous nucleation are the foreign inclusions and surface oxides.

During flight, the droplet exchanges its thermal energy with the atomization gas and cools to below the liquidus temperature. Nucleation occurs at a certain temperature below the liquidus temperature. This study provided evidence of the occurrence of several nucleation events for each droplet. Based on microstructural observations, it was assumed that there are six nucleation events uniformly distributed on the surface of each droplet irrespective of its size. Following nucleation, growth completes the crystallization of the undercooled melt. The crystallization is considered to be over once the sum of the volumes of the growing nuclei is equal to the volume of the droplet, i.e., the overall extended volume fraction is equal to one. For aluminum alloy 7150, the solidification does not occur at a single temperature but over a range of temperatures. Immediately following nucleation occurs recalescence, which results from the release of latent heat during solidification. The onset of nucleation, or the degree of undercooling, is determined by the catalytic ability of heterogeneous centers and the cooling rate experienced by the droplet. At the end of recalescence, the temperature of the droplet increases and approaches the equilibrium transformation temperature.

For the case of spray forming, the oxidation of the surfaces of the droplet and the deposited material's surface is minimized since the experiments were conducted inside an inert gas environment. The absence of prior droplet boundaries within the droplet material strongly supports the premise that a metallurgical bond has developed between the impinging droplets and the previously deposited material. Further, the droplets impinge and spread at a high speed on the previously deposited surface material's surface. These competing factors suggest that the interfacial heat transfer coefficient between the impinging droplets and the previously deposited material in spray forming is likely to be higher than those associated with the planar casting and droplet-splat processes. This interference is justified by the fact that a metallurgical bond between the impinging droplets and the previously deposited material is mandatory in the spray forming process [210].

The temperature at the deposited material's surface constantly increases with its thickness, and exceeds the solidus temperature at a critical distance above the

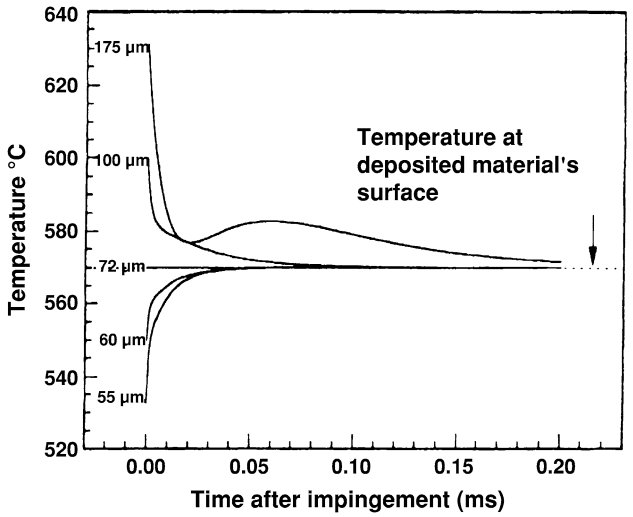

Fig. 34 Temperature history of individual droplets after they impinge on the surface of the deposited material at 570 °C with an interfacial heat transfer coefficient of 10^7 W m^{-2} K^{-1} [210]

substrate. Following this region, the deposited material's surface is in a mushy state. After the mushy layer forms, no second nucleation occurs and the remaining liquid of incoming droplets is exhausted during the growth of the existent nuclei. When a droplet impinges on the mushy surface, two phenomena tend to occur (Fig. 34). When the temperature of the droplet is higher than the temperature at the deposited material's surface, the droplet is quickly quenched down to the temperature of the deposited materials' surface. Correspondingly, the nuclei contained within the droplet generated during flight accelerate their growth to a certain size, which is dictated by the current temperature at the surface of the deposited material. On the contrary, if the temperature of the impinging droplet is lower than the temperature at the surface of the deposited material, the droplet is quickly heated to the temperature at the surface of the deposited material. In response to this temperature change, for a partially solidified droplet, the nuclei will terminate their growth and rapidly shrink by remelting to a certain size, which is determined by the current temperature. However, for a fully solidified droplet, it will remelt, and the cooling process of the mushy layer determines its re-solidification. Thus, the deposited material's surface behaves like a size modulator, which has the tendency to homogenize the different size nuclei contained within a diversity of impinging droplets within a short span of time.

For the aluminum alloy, 7150 examined in this study the microstructure was not characterized by equiaxed grain morphology but grains whose sizes are significantly different. Regions of small grains were judiciously dispersed between regions of large grains. The microstructure of the deposited alloy both at and away from the substrate is shown in Fig. 35.

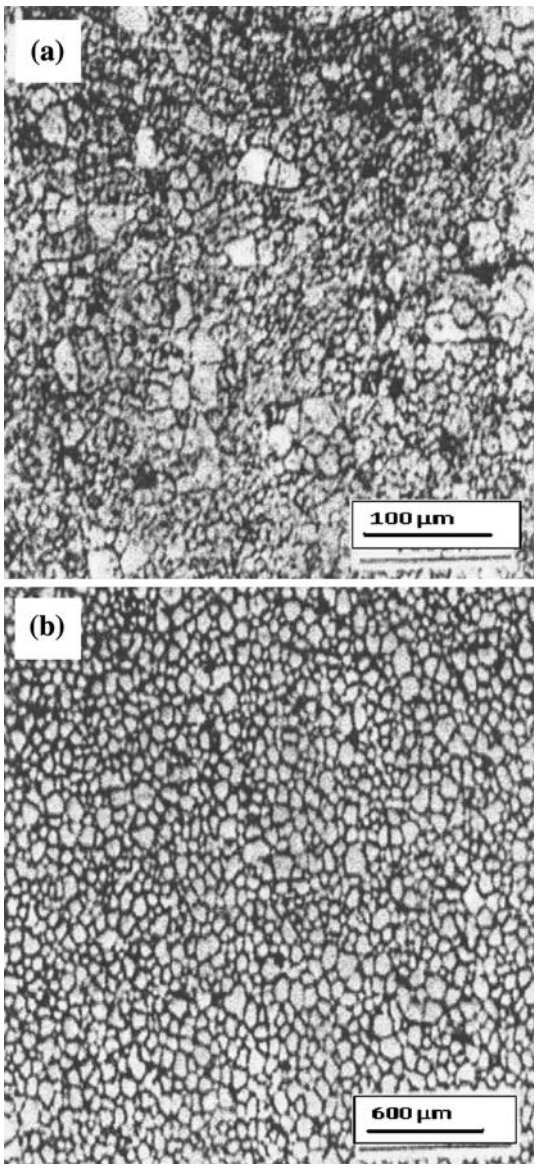

Fig. 35 Microstructure of the deposited aluminum alloy 7150: **a** at 3 mm away from the substrate, **b** at the region approximately 100 mm away from the substrate [210]

Conclusions

The wide body of literature that is reviewed in this technical manuscript on RSP of materials focuses on the basic science of the process, the principles governing operation of a specific technique, technological viability, and potential commercial applications. A variety of commercially viable and economically affordable RSP techniques is presented and their salient aspects or features

highlighted. The results documented in the open literature have most certainly enriched our understanding of the inter-relationship between processing science and variables with microstructural development and its concomitant influence on mechanical properties or response of the material. The potential limitations of each technique that constrain its exhaustive use are highlighted.

Of the various processing techniques that have been tried on the emerging generation of materials, the technique of spray processing has gained increased attention and interest. Of the commercially viable spray processing techniques, the spray atomization and deposition technique offers several advantages over the competing techniques in terms of microstructural stability and refinement, property enhancement and overall efficiency of the process. The attractive combinations of microstructure and properties exhibited by the spray atomized and deposited materials have resulted from an overall compactness of the process, the intrinsic flexibility in controlling process parameters or variables, and a minimization or elimination of contaminants, particularly oxide contamination. The intricacies pertaining to advances in the use of the spray processing technique for the emerging generation of materials is discussed with five specific examples. Sustained efforts at attempting to both synergize and concurrently model several of the newer generation materials coupled with innovations in processing techniques are expected to be the key areas that will rapidly accelerate the technical viability and economics of RSP for the emerging technologies. The authors believe that while the science and related technology of RSP has reached an advanced stage, incremental advances or perturbation in both operation and use of this processing technique can extend its use for the synthesis of difficult to process materials.

Acknowledgements The authors (EJL and TSS) extend most sincere thanks, appreciation, and boundless gratitude to the "unknown reviewer" for his useful comments, corrections and suggestions, which have been carefully incorporated in the revised version of this manuscript. One of the authors (TSS) extends thanks and appreciation to Mr. Udaykar, B. for his timely assistance with preparing the figures in conformance with required specification.

References

1. Savage SJ, Froes FH (1984) J Met 36(4):20
2. Duwez P, Willens RH, Klement W (1960) J Appl Phys 31:1136
3. Duwez P, Willens RH, Klement W (1960) J Appl Phys 31:1146
4. Klement W, Willens RH, Duwez P (1960) Nature 187:869
5. Gilman JJ, Leamy HJ (eds) (1978) Metallic Glasses 1978. American Society for Materials International, Materials Park, Ohio
6. Jones H (1982) Rapid solidification of metals and alloys: monograph no. 8. The Institution of Metallurgists, London
7. Herman H (ed) (1981) Ultra rapid quenching of liquid alloys. Academic Press, New York
8. Ashbrook RL (ed) (1983) Rapid solidification technology: sourcebook. American Society for Materials International, Metals Park, Ohio
9. Ananthraman TR (ed) (1984) Metallic glasses: production, properties and applications. Trans Tech Publications, Aedermannsdorf
10. Flinn JE (1985) Rapid solidification technology for reduced consumption of strategic materials. Noyes Publication, Park Ridge, New York
11. Ananthraman TR, Suryanarayana C (1987) Rapidly solidified metals: a technological overview. Trans Tech Publications, Aedermannsdorf
12. Srivatsan TS, Sudarshan TS (1991) Rapid solidification technology: an engineering guide. Marcel Dekker Publications, New York
13. Das SK, Kear BH, Adam CM (eds) (1985) Rapidly solidified crystalline alloys. The Metallurgical Society of AIME, Warrendale, PA
14. Sastry SML, MacDonald BA (eds) (1986) Mechanical behavior of rapidly solidified materials. The Metallurgical Society of AIME, Warrendale, PA
15. Giessen BC, Polk DE, Taub AI (eds) (1986) In: Materials research society symposium proceedings, vol 58, Boston, MA
16. Froes FH, Savage SJ (eds) (1987) Processing of structural metals by rapid solidification. American Society for Materials International, Metals Park, Ohio
17. Lee PW, Carbonara RS (eds) (1988) Rapidly solidified materials. American Society for Materials International, Metals Park, Ohio
18. Mehrabian R, Parrish PA (eds) (1988) Rapid solidification processing: principles and technologies IV. Claitors Publication Division, Baton Rouge, Louisiana
19. Lee PW, Moll JH (eds) (1988) Rapidly solidified materials: processing and properties. American Society for Materials International, Metals Park, Ohio
20. Duwez P (1968) In: Bunshah RF (ed) Techniques of metals research, vol I. Interscience Publishers, New York, p 347
21. Pond RB, Maringer RE, Mobley CE (1976) New trends in materials fabrication. American Society for Metals, Metals Park, Ohio, p 128
22. Grant NJ (1978) In: Mehrabian R, Kear BH, Cohen M (eds) Rapid solidification processing: principles and technologies. Claitors Publications, Louisiana, p 230
23. Maringer RE, Mobley EC (1979) Wire J 12(21):70
24. Jones H (1981) In: Herman H (ed) Ultrarapid quenching of liquid alloys, treatise on materials science and technology, vol 20. Academic Press, New York, p 1
25. Jones H (1982) Rapid solidification of metals and alloys. The Institution of Metallurgists, London
26. Suryanarayana C, Froes FH, Rowe RG (1991) Int Mater Rev 36(3):85
27. Lavernia EJ, Ayers JD, Srivatsan TS (1992) Int Mater Rev 37:1
28. Armster SQ, Delplanque PP, Rein M, Lavernia EJ (2002) Int Mater Rev 47(6):1
29. Lewis RE, PalmerIG, Eckvall JC, Sakata IF, Quist WE (1983) In: Proceedings of the third international conference on rapid solidification processing, Gaithersburg, MD, December 1982. National Bureau of Standards, Washington, DC, p 613
30. Cohen M, Kear BH, Mehrabian R (1989) In: Mehrabian R, Kear BH, Cohen M (eds) Rapid solidification processing: principles and technologies II. Claitor Publishing Division, Baton Rouge, LA, p 1
31. Perepezco JH, Furrer DV, Mueller BA (1988) Annual meeting of The Minerals, Metals and Materials Society (TMS), February 1988, Phoeniz, Arizona

32. Jones H (1988) In: Kim YW, Griffith WM (eds) Dispersion Strengthened Aluminum Alloys. The Minerals, Metals and Materials Society, Warrendale, PA, p 57
33. Cochrane RF, Evans DV, Greer DV (1988) J Mater Sci Eng 98:99
34. Willnecker R, Herlach DM, Feuerbacher B (1988) J Mater Sci Eng 98:85
35. Jones H (1987) In: Froes FH, Savage SJ (eds) Processing of structural metals by rapid solidification. American Society for Metals, Metals Park, Ohio, p 77
36. Matyja H, Geissen BC, Grant NJ (1968) J Inst Met 96:30
37. Sarin VK, Grant NJ (1972) Metall Trans 3A:875
38. Grant NJ (1978) A review of various atomization processes. In: Mehrabian R, Kear BH (eds) Rapid solidification processing: principles and technologies. Claitors Publication Division, Baton Rouge, LA, p 230
39. Klar E, Shaefer WM (1972) In: Burke JJ, Weiss V (eds) Powder metallurgy for high performance applications. Syracuse University Press, Syracuse, NY, p 57
40. Dombrowski N, John WR (1963) Chem Eng Sci 118:203
41. A. Lawley (1983) In: Ashbrook RL (eds) Rapid solidification technology: source book. American Society for Metals, Materials Park, Ohio, p 47
42. Lee JB, Johnston GH (1978) Powder Technol 21:119
43. Hirschorn JS (1969) Introduction to powder metallurgy. American Powder Metallurgy Institute, New York, NY
44. Gummeson PU (1972) Powder Metall 15:67
45. Singer ARE, Coombs JS, Leatham AG (1974) In: Housner HH, Smith WE (eds) Modern developments in powder metallurgy, vol 8. Plenum Publishing House, New York, p 263
46. Shinde SL, Tenkoldar GS (1977) Powder Metall Int 9:132
47. Tallmadge JA (1978) In: Kuhn H, Lawley A (eds) Powder metallurgy processing: new techniques and analyses. Academic Press, New York
48. Klar E, Resko JW (1984) Powder metallurgy metal handbook, vol 7, 9th edn. American Society for Materials, Materials Park, Ohio, p 25
49. Rai G, Lavernia EJ, Grant NJ (1985) J Met 37:17
50. Couper MJ, Singerand RF (1985) In: Steeb S, Warlimont H (eds) Proceedings of the fifth international conference on rapidly quenched metals. North Holland Publishing House, Amsterdam, The Netherlands
51. Veistinen M, Lavernia EJ, Abinante M, Grant NJ (1987) Mater Lett 5(10):373
52. Baram J, Veistinen M, Lavernia EJ, Anbinante M, Grant NJ (1988) J Mater Sci 23:2457. doi:10.1007/BF01111903
53. Baram J (1988) Mater Sci Eng 98:65
54. Thompson JS (1948) J Inst Met 7:101
55. Libera M (1987) Doctor of Science Thesis, Massachusetts Institute of Technology, June
56. Perepezko JH (1984) Mater Sci Eng 65:125
57. McDonnell VG, Lavernia EJ, Samuelsen GS (1989) Proceedings of the annual meeting of The Minerals, Metals and Materials Society (TMS), February 28–March 3, Las Vegas, Nevada
58. Flemings MC (1974) Solidification processing, chap 3. McGraw Hill Publishers, New York
59. Salas O, Levi CG (1988) Int J Rapid Solidif 4:1
60. Bower TF, Brody HD, Flemings MC (1965) Trans AIME 233:624
61. Levi CG, Mehrabian R (1982) Metall Trans 13A:221
62. Lavernia EJ, Gutierrez E, Szekely J, Grant NJ (1987) In: Proceedings of the 1987 annual powder metallurgy congress and exhibition. Progress in powder metallurgy, vol 43, p 683
63. Lavernia EJ, Gutiuerrez E, Szekely J, Grant NJ (1988) Int J Rapid Solidif 4(1, 2):89
64. Gutierrez E, Lavernia EJ, Trapaga G, Szekely J, Grant NJ (1989) Metall Trans A 20A:71
65. Lubanska H (1970) J Met 22:45
66. Duwez P, Willens RH, Klement W (1960) J Appl Phys 31:1500
67. Predeck P, Mullendore AW, Grant NJ (1965) Trans Metall Soc AIME 233:1581
68. Miroshnichenko IS, Salli IV (1959) Ind Lab 25:1463 (From (1959) Zavodskaya Lab 25:1398)
69. Mobley CE (1971) Metallurgy and Applications of Rapid Solidification. Battelle Seattle Research Center, Seattle, WA
70. Mobley CE, Clauer AH, Wilcox B (1972) J Inst Met 100:142
71. Strange EH (1911) United States Patent Number 993,904, Granted in 1911
72. Jones H (1969–1970) J Mater Sci Eng 5:1
73. Chu ME, Diron A, Granger DA (1985) In: Lee PW, Carbonara RS (eds) Rapidly solidified materials. American Society for Materials, Materials Park, p 311
74. Bewlay BP, Cantor B (1986) Int J Rapid Solidif 2:107
75. Collins LE (1986) Can Metall Q 25(1):59
76. Haour G, Boswell P (1987) Mater Des 8(1):10
77. Gutierrez Miravete E (1991) In: Srivatsan TS, Sudarshan TS (eds) Rapid solidification technology, an engineering guide. Marcel Dekker Publications, New York, p 3
78. Singer ARE, Evans RW (1983) Met Technol 10(2):61
79. Lavernia EJ, Wu Y (1996) Spray atomization and deposition. Wiley, New York. ISBN 0-471-95477-2
80. Perepezko JH (1988) In: Nucleation kinetics: casting, vol 15A. ASM Metals Handbook, Metals Park, OH, p 101
81. Lee JK, Aaronson HI (1975) In: Aaronson HI (ed) Lectures on the theory of phase transformations. The Metallurgical Society, Warrendale, PA, p 83
82. Lesoult G (1988) Fundamentals of growth in casting, vol 15A. ASM Metals Handbook, p 109
83. Christian JW (1975) Chapter 10 in the theory of transformation in metals and alloys: part 1, 2nd edn. Pergamon Press, Oxford
84. Turnbull D (1969) Contemp Phys 10(5):473
85. Chen HS (1980) Rep Prog Phys 43:353
86. Argon AS (1982) J Phys Chem Solids 43(10):945
87. Gilmer GH (1984) Mater Sci Eng 65:15
88. Flemings MC (1974) Chapter 2 in solidification processing. McGraw Hill Publishing House, New York
89. Baker JC, Cahn JW (1971) Solidification. American Society for Metals, Metals Park, Ohio, p 23
90. Flemings MC (1981) In: Tien JK, Elliott JF (eds) Metallurgical treatises. The Metallurgical Society of AIME, Warrendale, PA, p 291
91. Rack HJ, Baruch TR, Cook JL (1980) In: Hasyadhi T, Kawata K, Umekawa S (eds) Science and engineering of composite materials. Japan Society for Composite Materials, Tokyo, p 1465
92. Rack HJ, Niskanen PW (1984) Light Met Age February:9
93. Chawla KK (1985) J Met 37:25
94. Rack HJ, Ratnaparkhi P (1988) J Met 40:55
95. Rack HJ (1988) Adv Mater Manuf Process 3(3):327
96. Hunt WH Jr, Cook CR, Armanie KP, Garganus TB (1987) In: Kumar P, Ritter A, Vedula K (eds) Powder metallurgy composites. Metallurgical Society of AIME, Warrendale, PA
97. Geiger AL, Walker JA (1991) J Met 43:8
98. Marcus HL, Bournell DL, Eliezer Z, Prasad C, Weldon WF (1987) J Met 12
99. Elkabir G, Rakenberg LK, Prasad CV, Marcus HL (1986) Scr Metall 20(10):1411
100. Cebulak WS, Johnson EW, Marcus HL (1976) Mater Eng Q 16(4):37
101. Harrigan WC (1984) In: Sixth annual conference on discontinuously-reinforced aluminum composite. Material Coordination Working Group, Park City, Utah, January

102. Raybould D, Morris DG, Cooper GA (1979) J Mater Sci 14:2523. doi:10.1007/BF00737047
103. Morris DG (1982) In: Masumoto T, Suzuki K (eds) Proceedings of the fifth conference on rapidly quenched metals, vol 1. Japan Institute of Metals, Sendai, Japan, p 145
104. Morris DG (1986) In: Mehrabian R, Kear BH, Cohen M (eds) Second international conference on rapid solidification processing. Claitoirs Publishing Division, Baton Rouge, LA, p 1
105. Cline CF, Hopper RW (1977) Scr Metall 11:1137
106. Morris DG (1980) Mater Sci 14:215
107. Iyer NC, Fine DA, Male AT (1984) In: Berman I, Schroeder JW (eds) Proceedings of the eighth international conference on high energy rate fabrication, San Antonio, Texas, p 137
108. Grant NJ, Pelloux RM (1972) In: Proceedings of the first army materials technology conference. Metals and Ceramics Information Center, Columbus, Ohio, p 317
109. Lenel FV (1980) Metal powder industries federation. Princeton, New Jersey, p 321
110. Lenel FV, Ansell GS (1982) J Met 34:17
111. Nueing HC (1982) Powder Metall 25(3):160
112. Morgan JT, Begel H, Doraivelu SM, Matson L, Martorell I, Thomas JF (1982) In: Koczak MJ, Hildeman GJ (eds) High strength powder metallurgy aluminum alloys. The Minerals, Metals and Materials Society, Warrendale, PA, p 193
113. Griffith WM, Kim YW, Fries FH (1986) In: Fine ME, Starke EA Jr (eds) Rapidly solidified powder aluminum alloys, ASTM STP 890. ASTM Publications, Philadelphia, PA, p 283
114. James WB (1985) Int J Powder Metall Powder Technol 21(3):163
115. Cahn HW, Dunham DP, Gibeling JC (1988) J Met 40
116. Raybould D, Morris DG, Cooper GA (1979) J Mater Sci Lett 14:1011
117. Morris DG (1981) Met Sci 15:116
118. Morris DG (1983) Mater Sci Eng 57:187
119. Peng TC, Sastry SML, O'Neal JE, Brasher D (1985) Metall Trans A 16A:1445
120. Gupta M, Mohamed FA, Lavernia EJ (1989) In: Mostaghci H (ed) Proceedings of the international symposium on advances in processing and characterization of ceramic-metal composites, CIM/ICM, vol 17. Pergamon Press, Oxford, p 236
121. Gupta M, Mohamed FA, Lavernia EJ (1990) Mater Manuf Process 5(2):165
122. Bricknell RH (1986) Metall Trans 17A:583
123. Fiedler HC, Sawyer TF, Koop RW, Leatham AG Jr (1987) J Met 39(8):28
124. Zhang LZ, Majewska-Glabus I, Vetter R, Duszcyk J (1990) Scr Metall 24(11):2025
125. Kojima KA, Lewis RE, Kaufman MJ (1989) In: Sanders TH Jr, Starke EA Jr (ed) Aluminum-lithium alloys V. Materials and Component Engineering Publications, Birmingham, p 85
126. Lavernia EJ (1989) Int J Rapid Solidif 5:47
127. Willis TC (1988) Met Mater 4:485
128. Singer ARE, Ozbek S (1985) Powder Metall 28(2):72
129. Grant PS, Kim WY, Bewlay BP, Cantor B (1989) Scr Metall 23:1651
130. Moran AL, Palko WA (1988) J Met 40(12):12
131. Gutierrez E, Lavernia EJ, Trapaga G, Szekely J, Grant NJ (1989) Metall Trans 20A:71
132. Srivatsan TS, Lavernia EJ (1993) In: Ravi VA, Srivatsan TS (eds) Processing and fabrication of advanced materials for high temperature applications II. The Minerals, Metals and Materials Society, Warrendale, PA, p 141
133. Gupta M, Mohamed FA, Lavernia EJ, Srivatsan TS (1993) J Mater Sci 28:2245. doi:10.1007/BF00367591
134. Apelian D, Wei D, Farouk B (1989) Metall Trans B 20:251
135. Xu Yue, Lavernia EJ (1993) In: Ravi VA, Srivatsan TS, Moore JJ (eds) Processing and fabrication of advanced materials III. The Minerals, Metals and Materials Society, Warrendale, PA
136. Zeng X, Nutt SR, Lavernia EJ (1993) In: Ravi VA, Srivatsan TS, Moore JJ (eds) Processing and fabrication of advanced materials III. The Minerals, Metals and Materials Society, Warrendale, PA
137. Zhang Q, Rangel RH, Lavernia EJ (1996) Acta Mater 44(9): 3693
138. Sampath S, Gudmundsson B, Tiwari R, Herman H (1988) Proceedings of the third national thermal spray conference, Cincinnati, October. ASM International, Metals Park, Ohio
139. Tiwari, Herman H, Sampath S, Gudmundsson B (1991) In: Fishman SG (ed) Proceedings of the symposium on innovative inorganic composites. The Minerals, Metals and Materials Society, Warrendale, PA
140. Sampath S, Tiwari R, Gudmundsson B, Herman H (1991) Scr Metall 25:1425
141. Buhrmaster CL, Clark DE, Smartt HB (1988) J Met 40:44
142. Parker DW, Kutner GL (1991) Adv Mater Process 149:68
143. Buzby PO, Nikitich J (1991) Adv Mater Process 149:35
144. Singer ARE (1970) Met Mater 4:246
145. Singer AR (1972) J Inst Met 100:185
146. Daugherty TS (1968) Powder Metall 2:342
147. Brooks RG, Leatham AG, Coombs JS, Moore C (1977) Metall Met Form 9:1
148. Williams B (1980) Met Powder Rep 10:464
149. Brooks RG, Moore C, Leatham AG, Coombs JS (1977) Powder Metall 2:100
150. Dube RK (1982) Powder Metall Int 14:108
151. Evans RW, Leatham AG, Brooks RG (1985) Powder Metall 28(1):13
152. Leatham AG, Brooks RG (1984) Mod Dev Powder Metall 15:157
153. Ogilvy AJ, Chesney PF, Metelman O (1988) Mod Dev Powder Metall 18–21:475
154. White J, Hughes IR, Willis TS, Jordon RM (1987) In: Aluminum lithium conference proceedings, Paris, France, June
155. Willis TC, White J, Jordon RM, Hughes IR (1988) The microstructure and properties of aluminum-SiC composite material produced by spray deposition. Solidification processing conference. The Institute of Metals, London
156. White J, Willis TC, Hughes IR, Palmer IG, Jordon RM (1988) In: Kim YW, Griffith WM (eds) Dispersion strengthened aluminum alloys. The Minerals, Metals and Materials Society, Warrendale, PA, p 693
157. Ibrahim IA, Mohamed FA, Lavernia EJ (1991) J Mater Sci 26:1137. doi:10.1007/BF00544448
158. Ibrahim IA, Mohamed FA, Lavernia EJ (1990) In: Khan T, Effenberg G (eds) International conference on advanced aluminum sand magnesium alloys. ASM International, Amsterdam, The Netherlands, p 745
159. Ast DG, Zielinski PG (1982) In: Proceedings of the third international conference on rapid solidification processing, Gaithersburg, Maryland, p 384
160. Annavarapu S, Apelian D, Lawley A (1988) Metall Trans 198A:3077
161. Gupta M, Mohamed FA, Lavernia EJ (1991) Int J Rapid Solidif 6:247
162. Liang X, Lavernia EJ (1992) Mater Sci Eng A153:646
163. Liang X, Lavernia EJ (1991) Scr Metall Mater 25:1199
164. Cahn RW (1991) MRS Bull 5:18
165. Stoloff N (1989) Int Mater Rev 34:153
166. Liang X, Earthman JC, Wolfenstine J, Lavernia EJ (1992) Mater Charact 28:3003
167. Chigier NA (1991) In: Proceedings I-CLASS 91, NIST. US Department of Commerce, July 15–18, 1991, p 1

168. LeFebvre AH (1991) In: Proceedings I-CLASS-91, NIST. US Department of Commerce, July 15–18, 1991, p 49
169. Lupis CHP (1983) Chemical thermodynamics of materials. Elsevier, New York, p 345
170. Turnbull D (1987) In: Collins EW, Koch CC (eds) Undercooled alloy phases. AIME-TMS, Warrendale, PA, p 3
171. Annavarapu S, Apelian D, Lawley A (1990) Metall Trans A 21:3237
172. Zhuang LZ, Majewskja-Glabus I, Vetter R, Duszezyk J (1990) Scr Metall Mater 24:2083
173. Liang X, Kim H, Earthman JC, Lavernia EJ (1992) Mater Sci Eng A 152:646
174. Gupta M, Mohamed F, Lavernia EJ (1992) Metall Trans A 23:831
175. Gupta M, Mohamed F, Lavernia EJ (1992) Metall Trans A 23A:844
176. Lavernia EJ, Wu Y, Xu Q, Srivatsan TS (2000) In: Proceedings of the third international conference on advances in composites, ADCOMP 2000, August 2000, Bangalore, India
177. Singer ARE (1988) In: Sahai Y, Battles JE, Carbonara RS, Mobley CE (eds) Casting of near shape products. TMS-AIME, Warrendale, PA, p 245
178. Annavarapu S, Apelian D, Lawley A (1988) Metall Trans 19A:3077
179. Mathur P, Apelian D, Lawley A (1989) Acta Metall 37:429
180. Liang X, Earthman JC, Lavernia EJ (1992) Acta Metall Mater 40(121):3003
181. Liang X, Lavernia EJ (1993) Mater Sci Eng A 161:221
182. Liang X (1991) Doctor of Philosophy Thesis, University of California at Irvine, Irvine, CA
183. Kruz W, Fisher DJ (1986) Fundamentals of solidification. Trans Tech Publications, Switzerland, p 9
184. Davies GJ (1973) Solidification and casting. Halsted Press, Wiley Publishing, New York, p 25
185. Evans RW, Leathman AG, Brooks RG (1985) Powder Metall 28:13
186. Singer ARE (1986) Met Powder Rep 3:223
187. Apelian D, Wei D, Farouk B (1989) Metall Trans 20B:251
188. Srivatsan TS, Lavernia EJ (1992) J Mater Sci 27:5965. doi: 10.1007/BF01133739
189. Sampath S, Herman H (1988) In: Houck DL (ed) Thermal spraying advances in coatings technology. ASM International, Materials Park, Ohio, p 1
190. Gupta M, Mohamed FA, Lavernia EJ (1992) Scr Metall Mater 26:697
191. Flemings MC, Mortensen A (1984) Army Materials Laboratory final report AMMRC 7R 84-37, AD-A 150270, September
192. Meschter PJ, O'Neil JE (1984) Metall Trans 15A:237
193. Das SK, Davis LA (1988) Mater Sci Eng 98:1
194. Lavernia EJ, Baram J, Gutierrez E (1991) Mater Sci Eng A 132:119
195. Foerster GS (1972) Metall Eng Q 12(1):22
196. Leimkuhler Motramn A, Palko WA (1987) Prog Powder Metall 43:711
197. Bewlay P, Cantor B (1986) In: Lee P, Carbonara RS (eds) Proceedings of the ASM international conference on rapidly solidified materials. ASM Metals Park, Ohio, p 15
198. Ruhr M, Lavernia EJ, Baram J (1990) Metall Trans 21A:1785
199. Lavernia EJ, Gutierrez E, Szekely J, Grant NJ (1988) Int J Rapid Solidif 4(1–2):89
200. Lavernia EJ, Gutierrez E, Szekely J, Grant NJ (1987) Prog Powder Metall 43:683
201. Gutierrez E, Lavernia EJ, Trapaga G, Szekely J (1988) Int J Rapid Solidif 4(1–2):125
202. Gutierrez E, Lavernia EJ, Trapaga G, Szekely J, Grant NJ (1989) Metall Trans A 20:71
203. Kujha H, Lawley A (1978) Powder metallurgy processing: new techniques and analysis. Academic Press, New York
204. Savitskii EM (1969) Palladium alloys. Primary Sources, New York, NY
205. Field RD, Thoma DJ (1997) Scr Mater 37:347
206. Timofeyev NI, Bereseneva FN (1991) Phys Met Metall 72:147
207. Yang N, Bing Li, Robinson S, Lavernia EJ (2000) Metall Mater Trans 31A:1843
208. Yang N, Guthrie SE, Ho S, Lavernia EJ (1996) J Mater Syn Process 4(1)
209. Kurz W, Fisher DJ (1986) Fundamentals of solidification. Trans Tech Publications, Aedermannsdorf, Switzerland
210. Xu Q, Lavernia EJ (2001) Acta Mater 49:3849